nature cell biology

The prolyl-isomerase Pin1 is a Notch1 target that enhances Notch1 activation in cancer

Alessandra Rustighi[1,8], Luca Tiberi[1,8], Alessia Soldano[1], Marco Napoli[1], Paolo Nuciforo[2], Antonio Rosato[3,4], Fred Kaplan[5], Anthony Capobianco[5], Salvatore Pece[2,6], Pier Paolo Di Fiore[2,6,7] and Giannino Del Sal[1,9]

Signalling through Notch receptors requires ligand-induced cleavage to release the intracellular domain, which acts as a transcriptional activator in the nucleus. Deregulated Notch1 signalling has been implicated in mammary tumorigenesis; however the mechanisms underlying Notch activation in breast cancer remain unclear. Here, we demonstrate that the prolyl-isomerase Pin1 interacts with Notch1 and affects Notch1 activation. Pin1 potentiates Notch1 cleavage by γ-secretase, leading to an increased release of the active intracellular domain and ultimately enhancing Notch1 transcriptional and tumorigenic activity. We found that Notch1 directly induces transcription of Pin1, thereby generating a positive loop. In human breast cancers, we observed a strong correlation between Pin1 overexpression and high levels of activated Notch1. Thus, the molecular circuitry established by Notch1 and Pin1 may have a key role in cancer.

Notch signalling is central for regulation of cell fate, maintenance of stem-cell populations and differentiation. Indeed, impairment of Notch signalling has been linked to various developmental disorders and to carcinogenesis[1,2]. Following interaction with its ligands, membrane-bound Notch undergoes two proteolytic cleavages. The first is catalysed by an extracellular ADAM metalloprotease, and the second is catalysed by γ-secretase, releasing the Notch intracytoplasmic domain (NICD). NICD then translocates to the nucleus where, after interacting with CSL factors and transcriptional co-activators, it modulates the expression of target genes[3,4].

Alterations in Notch signalling have been reported in T-ALLs, which harbour Notch-activating translocations. Recently, Notch has been found to be deregulated in several carcinomas, including breast cancer[2,5]. Notch1 activation has been shown to be causally involved in the oncogenic conversion of human breast epithelial cells triggered by Wnt[6], and loss of Numb, a negative regulator of Notch1, has been observed in about 50% of breast carcinomas[7]. Oncogenic Ras activation, through the function of the MAPK/SAPK pathway, may also underlie deregulated Notch signalling in breast carcinomas[8]. Interestingly, attenuation of Notch1 signalling reverts the transformed phenotype of Ras-induced mammary tumours and of human breast cancer cell lines[9,10], suggesting that Notch could be a target for drug-based therapy of breast cancer[5,11].

Phosphorylation-dependent prolyl-isomerization catalysed by Pin1 is emerging as a potent mechanism in signal transduction[12,13]. Through its amino-terminal WW domain, Pin1 contacts phosphorylated Ser/Thr-Pro motifs contained in several substrates and catalyses *cis-trans* isomerization of the intervening peptide bond by means of its carboxy-terminal PPIase domain, resulting in conformational changes of its substrates[12,13]. Pin1 activity is crucial in the control of DNA damage checkpoint pathways, by regulating the functions of p53 (refs 14, 15) and p73 (ref. 16), but also modulates cell proliferation through stabilization of cyclin D1 (ref. 17), β-catenin[18], NF-κB[19] and several other proteins[12,13]. Pin1 is also involved in the regulation of APP, a γ-secretase substrate[20,21]. Finally, alterations of Pin1 have been implicated in the amplification of oncogenic signals[12,13], as shown by its cooperation with the Neu/Ras pathway in mammary tumorigenesis[22], and by its frequent deregulation in several human malignancies, including breast cancer[23,24].

Here, we show that Pin1 has a role in the activation of human Notch1, through modulation of its cleavage by γ-secretase. We found that Pin1 binds directly to Notch1 and regulates its activity, cooperating with Notch1 in tumorigenesis. Moreover, we show that Pin1 is itself a direct transcriptional Notch1 target, highlighting a feed-forward loop between these two factors. This circuitry may have relevance to human tumorigenesis, as shown by the strong correlation, observed in breast cancers, between Pin1 overexpression and the presence of high levels of activated Notch1 and of the Notch1 target HES-1.

[1]Laboratorio Nazionale CIB (LNCIB), Area Science Park, Padriciano 99, 34012 Trieste, Italy, and Dipartimento di Scienze della Vita, Università degli Studi di Trieste, via Giorgieri 1, 34128 Trieste, Italy. [2]Dipartimento di Medicina, Chirurgia ed Odontoiatria, Università di Milano, via di Rudinì 8, 20142 Milan, Italy. [3]Dipartimento di Scienze Oncologiche e Chirurgiche dell'Università di Padova, via Gattamelata 64, 35128 Padova, Italy. [4]Istituto Oncologico Veneto, IOV, via Gattamelata 64, 35128 Padova, Italy. [5]The Wistar Institute, 3601 Spruce Street, Philadelphia, Pennsylvania 19104, USA. [6]Istituto Europeo di Oncologia, via Ripamonti 435, 20141 Milan, Italy. [7]IFOM, the FIRC Institute for Molecular Oncology Foundation, via Adamello 16, 20139 Milan, Italy.
[8]These authors contributed equally to this work.
[9]Correspondence should be addressed to G.D.S. (e-mail: delsal@lncib.it)

Received 29 July 2008; accepted 22 October 2008; published online 18 January 2009; DOI: 10.1038/ncb1822

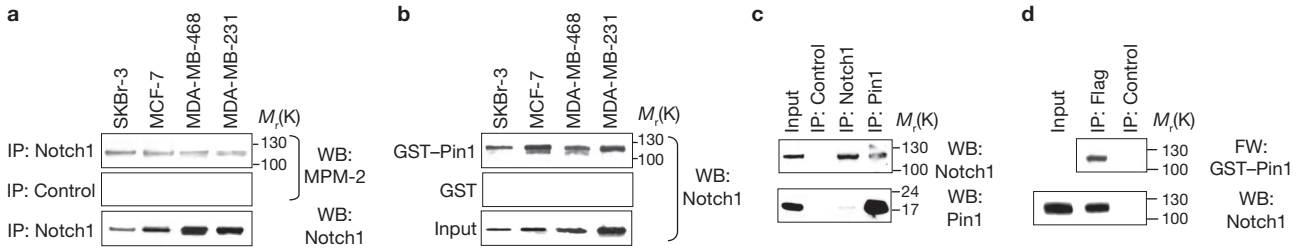

Figure 1 Pin1 binds to human Notch1. (**a**) Endogenous Notch1 is phophorylated at Ser/Thr-Pro sites. Control antibody or anti-Notch1 immunoprecipitates (IP) from the indicated cell lines were probed with anti-MPM-2 in western blots (WB), followed by stripping and anti-Notch1 western analysis to show immunoprecipitated protein levels. (**b**) Notch1 binds to Pin1. Lysates used in **a** were subjected to GST or GST–Pin1 pulldown followed by anti-Notch1 western blotting. The input lane shows 5% of total lysate. (**c**) Notch1 and Pin1 interaction occurs *in vivo*. Western blot analysis using control antibody, anti-Notch1 or anti-Pin1 co-immunoprecipitates from SKBr-3 cells. (**d**) Notch1 and Pin1 interaction is direct. Control or anti-Flag antibody immunoprecipitates from GSI-treated, pcDNA3-N1ΔE–Flag-transfected SKBr-3 cells, were subjected to far-western blotting using purified GST–Pin1 as a probe, followed by anti-Pin1 immunoblotting. Anti-Notch1 western blot analysis of the upper panel after stripping is shown.

RESULTS

Pin1 binds to Notch1 and modulates its function

The Notch1 cytoplasmic region harbours many Ser/Thr-Pro motifs, whose phosphorylation may generate Pin1-binding sites. Indeed, endogenous Notch1 expressed in breast cancer cell lines, was recognized by an anti-phospho-Ser/Thr-Pro (MPM-2) antibody (Fig. 1a) and bound to recombinant Pin1 *in vitro* (Fig. 1b). This interaction required a functional Pin1 WW domain and relied on phosphorylation of Notch1, as demonstrated by loss of binding when treated with phosphatases (Supplementary Information, Fig. S1a, b). Reciprocal co-immunoprecipitation (Fig. 1c) and far-western (Fig. 1d) assays demonstrated that Notch1 and Pin1 interaction occurs *in vivo* and is direct.

To test whether Pin1 could modulate the Notch1 pathway, we analysed induction of the Notch1 target HES-1 (ref. 25) in luciferase reporter assays. We overexpressed a membrane-tethered, ligand-independent Notch1 derivative (N1ΔE) that is constitutively cleaved by γ-secretase, releasing active N1ICD[26]. These assays showed that overexpression of wild-type Pin1, but not a catalytically inactive Pin1 mutant ($Pin1^{S67E}$; ref. 27), could enhance N1ΔE activity (Fig. 2a). Treatment with the γ-secretase inhibitor (GSI) DAPT abrogated the observed effect (Fig. 2a). Moreover, *Pin1* ablation by RNA interference (RNAi) or inhibition of its catalytic activity by the small molecule inhibitor PiB[28], significantly reduced *HES-1* promoter activation by N1ΔE (Fig. 2b, c). Together, these results indicate that Pin1 interacts with human Notch1 and regulates its pathway through prolyl-isomerase activity.

Pin1 affects Notch1 processing by γ-secretase

To determine how Pin1 was able to affect Notch1 signalling, we tested whether it modulates Notch1 processing by γ-secretase. Ablation of Pin1 in N1ΔE-transfected cells, with two different short interfering RNAs (siRNAs), resulted in decreased levels of processed N1ICD (Fig. 3a; Supplementary Information, Fig. S2a). We then analysed the effects of Pin1 overexpression on endogenous Notch1 processing by measuring the amount of N1ICD produced by EDTA treatment in culture. This treatment has been shown to trigger Notch1 cleavage by γ-secretase[29] and is blocked by GSI. Overexpression of Pin1 in human MCF-10A cells clearly increased Notch1 processing triggered by EDTA (Fig. 3b). Conversely, treatment with PiB (data not shown) or ablation of Pin1 reduced endogenous Notch1 cleavage after EDTA treatment in SKBr-3 cells (Supplementary Information Fig. S2b).

Finally, we measured EDTA-induced processing of Notch1 in $Pin1^{+/+}$ and $Pin1^{-/-}$ primary mouse embryo fibroblasts (MEFs)[30]. Lower levels of N1ICD were detected in $Pin1^{-/-}$ than in $Pin1^{+/+}$ cells (Fig. 3c), and also in presence of the proteasome inhibitor lactacystin (data not shown). Notch1 processing in $Pin1^{-/-}$ MEFs was completely rescued when wild-type Pin1 was re-introduced (Fig. 3c), suggesting that the observed effect was Pin1-dependent.

Pin1 enhances Notch1 cleavage through the Ser-Thr-rich (STR) region

To determine the mechanism by which Pin1 modulates Notch1 processing, we first mapped the Pin1-interacting domains on Notch1. Several N1ΔE deletion mutants were generated (Fig. 4a), overexpressed in GSI-treated HEK293T cells, and tested for binding to GST–Pin1 (WW) *in vitro*. Truncation of the C-terminal PEST domain (dP) reduced the interaction with Pin1, which was further decreased by deleting the TAD domain (d2171; Fig. 4b). Binding was abolished in d2120 with further removal of the STR region[31].

To identify which Pin1-interacting regions were important for Notch1 cleavage, we tested processing efficiency of all deletion mutants overexpressed in SKBr-3 cells. Only those mutants lacking the STR region (d2120, dSTR, dSTR-dP) showed reduced cleavage, compared with N1ΔE or d2171, which contain the STR region (Fig. 4c, compare lane 3 versus 4; Supplementary Information, Fig. S3a, compare lane 1 versus 2 and 3 versus 4).

These results suggest that on binding to the STR region, Pin1 could produce a conformational change favouring Notch1 cleavage by γ-secretase. This region contains four Ser/Thr-Pro motifs, putative MAPK/SAPK targets, which could be phosphorylated, as indicated by western blot analysis with the phospho-specific antibody MPM-2 (Supplementary Information Fig. S3b). Moreover, binding of d2171 to GST–Pin1 (WW) was reduced by treatment of cells with MEK/Erk or JNK kinase inhibitors (Fig. 4d; Supplementary Information Fig. S3c), suggesting that these kinases could be responsible for the interaction. Thus, we generated single and multiple point-mutants of these sites by Ala substitution, and observed reduced binding and processing of both the triple mutant d2171-3M (S2122A;T2133A;S2137A) and the quadruple mutant, which lacks all Pin1 binding sites (Fig. 4e, f). When overexpressed in $Pin1^{-/-}$ cells, cleavage of these mutants was not affected by Pin1 overexpression (Supplementary Information, Fig. S3d). More

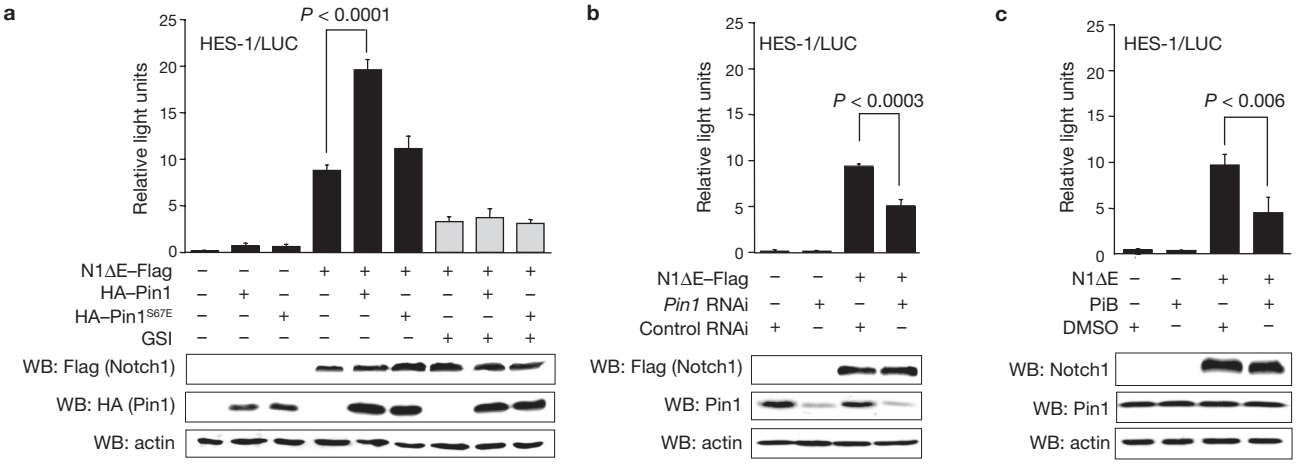

Figure 2 Pin1 affects Notch1 activity. (**a**) Pin1 enhances N1ΔE transcriptional activity. Luciferase assay in SKBr-3 cells co-transfected with pGL2HES-1/LUC and N1ΔE expression vector (pcDNA3-N1ΔE–Flag) along with expression vectors for either wild-type (HA–Pin1) or catalytically inactive (HA–Pin1^{S67E}) Pin1 is shown. Treatment with GSI (DAPT, 20 μM) is indicated (grey bars). (**b**) Specific knockdown of endogenous Pin1 affects Notch1 transcriptional activity. Transcriptional activity of N1ΔE was tested on HES-1/LUC in SKBr-3 cells in the presence of either a *Pin1*-specific (*Pin1* RNAi) or control siRNA. (**c**) The Pin1 inhibitor (PiB) reduces N1ΔE transcriptional activity. Luciferase assay of SKBr-3 cells co-transfected with HES-1/LUC and pcDNA3-N1ΔE–Flag and treated with PiB (0.5 μM) or vehicle. (**a**–**c**) Histograms represent mean ± s.d. of three independent experiments. *P* values are indicated for the observed differences. Cell lysates were analysed by western blotting and are shown below the histograms.

importantly, we tested the effect of mutation of these sites in the context of full-length N1ΔE (N1ΔE-3M) under the same conditions. Cleavage of N1ΔE but not N1ΔE-3M was sensitive to Pin1 overexpression (Fig. 4g). These data suggest that on Pin1 binding to crucial phosphorylated sites within the STR region, conformational changes are required for efficient cleavage by γ-secretase.

Pin1 potentiates Notch1 tumorigenic activity

The role of Pin1 in potentiating Notch1 signalling prompted us to investigate the effect of Pin1 on Notch1-transforming activity. N1ΔE was overexpressed in normal mammary MCF-10A cells, either alone or with HA–Pin1, and cells were tested for growth in soft agar. Consistent with a previous report[10], activated Notch1 was able to sustain anchorage-independent growth of these cells (Fig. 5a). Ectopic expression of Pin1 alone could not induce the formation of colonies in soft agar, but significantly increased colony-forming efficiency of N1ΔE (Fig. 5a). Ablation of *Pin1* by shRNA could block soft agar growth induced by N1ΔE, indicating that Pin1 is required for Notch1-induced cell transformation (Fig. 5a).

Western blot analysis of N1ΔE-expressing clones revealed that the levels of both cleaved Notch1 and the Notch1 target HES-1 were decreased when Pin1 was ablated (Fig. 5b, compare lanes 4 and 5). Conversely, their levels were enhanced by Pin1 overexpression (Fig. 5b, compare lanes 5 and 6). These results have also been confirmed in SKBr-3 cells. In this case, N1ΔE overexpression markedly increased the number of colonies exceeding a diameter of 100 μm; this was reduced by *Pin1* knockdown or treatment with PiB (Supplementary Information Fig. S4a, b, respectively).

We next tested whether the STR region, crucial for Notch1 processing efficiency, is important for its transforming activity. MDA-MB-231 breast cancer cells overexpressing N1ΔE, N1ΔE-dSTR or N1ΔE-3M were generated and assayed for anchorage-independent growth by scoring colonies exceeding a diameter of 100 μm. Deletion of STR or mutation of the crucial Pin1 binding sites (N1ΔE-3M), significantly reduced the transforming activity, compared with N1ΔE (Fig. 5c, d). In parallel, we tested the activity of nuclear N1ICD harbouring the same deletion (N1ICD-dSTR), but there was no significant reduction in colony number, compared with N1ICD-overexpressing cells (Fig. 5c). These results suggest that Pin1 affects Notch1-transforming activity in part by regulating its processing efficiency when acting on crucial phosphorylated sites within the STR region.

We also generated MDA-MB-231 cells overexpressing N1ΔE or N1ΔE-3M, along with vectors expressing *Pin1* or control shRNA (short hairpin RNA) and tested them as above (Supplementary Information, Fig. S4c). Consistent with our previous results, Pin1 downregulation markedly reduced N1ΔE-overexpressing colonies. However, Pin1 ablation also impaired, albeit to a lesser extent, the growth of N1ΔE-3M-overexpressing colonies, suggesting that the effect of Pin1 on growth could in part depend on its function on other substrates.

Finally we established MDA-MB-231 polyclonal populations overexpressing N1ΔE or empty vector together with *Pin1* shRNA, or *LacZ* shRNA as a control (Fig. 5e), and injected them subcutaneously into nu/nu mice to test the relevance of Pin1 on Notch1 tumorigenic activity *in vivo*. MDA-MB-231 cells are known to be tumorigenic *in vivo*; however overexpression of N1ΔE in MDA-MB-231 cells further increased their tumour growth, as shown by comparison with cells transfected with the empty vector (Fig. 5e). We observed that N1ΔE (*LacZ* shRNA)-overexpressing cells produced rapidly growing tumours and their final size was greater than that of control cells (empty + *LacZ* shRNA). Conversely, *Pin1* ablation (N1ΔE + *Pin1* shRNA) impaired growth of the tumours and their final size was reduced, indicating that Pin1 affects the growth-promoting functions of Notch1 *in vivo*.

Pin1 is a Notch1 target gene

In cells stably expressing N1ΔE, we consistently observed higher levels of endogenous Pin1 as compared with control cells (Fig. 5b, compare lanes 2 and 5; Supplementary Information, Fig. S4a, compare lanes 1 and 3). Notably, these increased Pin1 levels could be reversed by GSI treatment, as observed for the Notch1-target gene *HES-1* (Supplementary Information, Fig. S4a, compare lanes 3 and 6). This prompted us to

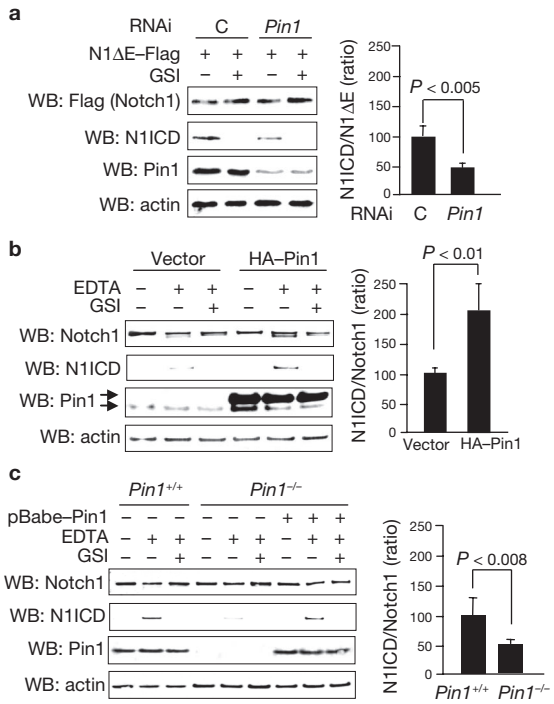

Figure 3 Pin1 affects Notch1 processing by γ-secretase. (**a**) Ablation of Pin1 impairs constitutive processing of N1ΔE. Western blot analysis of N1ΔE–Flag processing in SKBr-3 cells, transfected with control (C) or *Pin1* RNAi and treated with vehicle or GSI (DAPT, 20 μM) for 4 h, is shown. (**b**) Pin1 overexpression enhances Notch1 cleavage by γ-secretase. Western blot analysis of endogenous Notch1 processing from MCF-10A cells infected with pLPC (vector) or pLPC–HA–Pin1 and left untreated (–) or activated with EDTA (+), or EDTA and GSI as described previously[29]. Black arrows show migration of endogenous Pin1 (lower arrow) and overexpressed HA–Pin1 (upper arrow). (**c**) Notch1 processing decreases in *Pin1*$^{-/-}$ MEFs and is rescued by re-introduction of Pin1. Western blot analysis of *Pin1*$^{+/+}$ and *Pin1*$^{-/-}$ MEFs or *Pin1*$^{-/-}$ MEFs infected with a Pin1 retroviral expression vector (pBabe–Pin1) and mock-treated or treated with EDTA in **b**. Complete scans of the western blots are shown in Supplementary Information, Fig. S6. (**a**–**c**, right panels) Densitometric recording of cleaved (N1ICD) and uncleaved (N1ΔE or Notch1 untreated) protein levels was performed by Image J software and the ratio between N1ICD and the corresponding uncleaved form, was calculated. Shown are the mean ± s.d. of the ratios (percentage) from three independent experiments, setting the mean control ratio to 100% ± s.d.; *P* values for the observed differences are indicated.

investigate whether Notch1 could perturb endogenous Pin1 expression. To test whether Notch1 induces Pin1 at the transcriptional level, we performed semi-quantitative RT–PCR with MCF-7 cells overexpressing N1ICD and we observed increased *Pin1* mRNA levels, compared with vector-transfected cells (Fig. 6a).

Similarly, in H1299 cells expressing the N1ICD–ER[33] fusion protein[32], induction of N1ICD nuclear translocation by 4-OHT resulted in increased *Pin1* mRNA levels, similarly to those of Notch targets *HES-1* and *HEY-1* (Fig. 6b). These results are consistent with the presence of putative CSL-binding sites in the human *Pin1* promoter (Fig. 6c). We therefore cloned the *Pin1* promoter upstream of the luciferase gene and demonstrated that its activity was specifically induced by overexpression of N1ΔE (Fig. 6c). Chromatin immunoprecipitation (ChIP) analysis of MDA-MB-231 breast cancer cells demonstrated that the distal BS1 element on the *Pin1* promoter (also conserved in mouse) was specifically bound by endogenous N1ICD (Fig. 6d), whereas no chromatin association was detected after GSI treatment. This result was confirmed in HEK293T cells with endogenous Notch1 and in SKBr-3 cells with overexpression of N1ICD (data not shown).

N1ICD and Pin1 levels correlate in breast cancer

We analysed the levels of the Notch1 targets *Pin1* and *HES-1* in several breast tumour cell lines known to have deregulated Notch activity[10]. All showed high levels of both *HES-1* and *Pin1*, compared with normal breast MCF-10A cells (Fig. 7a).

These results suggest a cross-talk between Pin1 and Notch1 in breast carcinogenesis. To further investigate this possibility in primary breast cancers, we performed immunohistochemical analysis of Pin1 and N1ICD expression on serial sections from a breast tumour tissue microarray (TMA). This analysis highlighted a significant direct correlation between Pin1 expression levels and accumulation of N1ICD (Fig. 7b, c) as, in most cases (65%), tumours with high levels of nuclear N1ICD (59 out of 147) also had high levels of Pin1 protein levels, whereas low levels of N1ICD (88 out of 147) were paralleled by low levels of Pin1 (85%). Similar results were obtained from analysis of the levels of HES-1 and Pin1 on the same TMA (Fig. 7b, c).

Inhibition of γ-secretase and Pin1 reduces tumour growth

Our findings suggest that Pin1 and Notch1 are linked by a molecular circuitry. Indeed inhibition of Notch1 cleavage in different breast cancer cell lines by GSI treatment clearly reduced the levels of HES-1 and also Pin1 (Fig. 8a). To test the effect of combined inhibition of Notch1 and Pin1 on tumour cell growth in culture, we treated MDA-MB-231 cells with different concentrations of GSI after *Pin1* knockdown. The endogenous Notch1 pathway is activated in MDA-MB-231 cells[10,34] and, as already documented[35], treatment with GSI impedes growth of MDA-MB-231 cells after 6 days. We observed similar behaviour when these cells were treated with GSI (10 μM, Fig. 8b), whereas *Pin1* knockdown caused an even more marked reduction in growth. Intriguingly, administration of only 2 μM GSI in *Pin1*-ablated cells further reduced growth of these cells. Western blot analysis showed that in *Pin1*-silenced cells, 2 μM GSI treatment significantly reduced the levels of HES-1, similarly to 10 μM GSI-treated control cells. (Fig. 8b, lower panel, compare lanes 4 and 5). Similar results were obtained using GSI with PiB or *Pin1* shRNA expression (Supplementary Information Fig. S5a, b), supporting the notion that combined inhibition of Notch1 and Pin1 has a greater effect than either treatment alone on growth of cancer cells.

Finally, we orthotopically injected MDA-MB-231 cells expressing either *Pin1* or *LacZ* shRNA into the mammary fat pad of female immunocompromised mice and assessed tumour growth over several weeks (Fig. 8c). Consistent with the *in vitro* growth curves, ablation of endogenous *Pin1* significantly impaired tumour growth in this breast cancer xenograft model, further strengthening the pathophysiological relevance of this molecular circuitry in tumorigenesis.

DISCUSSION

Here we have demonstrated a role for Pin1 in enhancing human Notch1 signalling through its prolyl-isomerase activity. Pin1 interacts directly with phosphorylated Notch1 and increases Notch1 cleavage by γ-secretase. Accordingly, Pin1 contributes to Notch1 transforming properties both *in vitro* and *in vivo*. Notch1 in turn upregulates Pin1, thus establishing a feed-forward loop that amplifies Notch1 signalling. Our

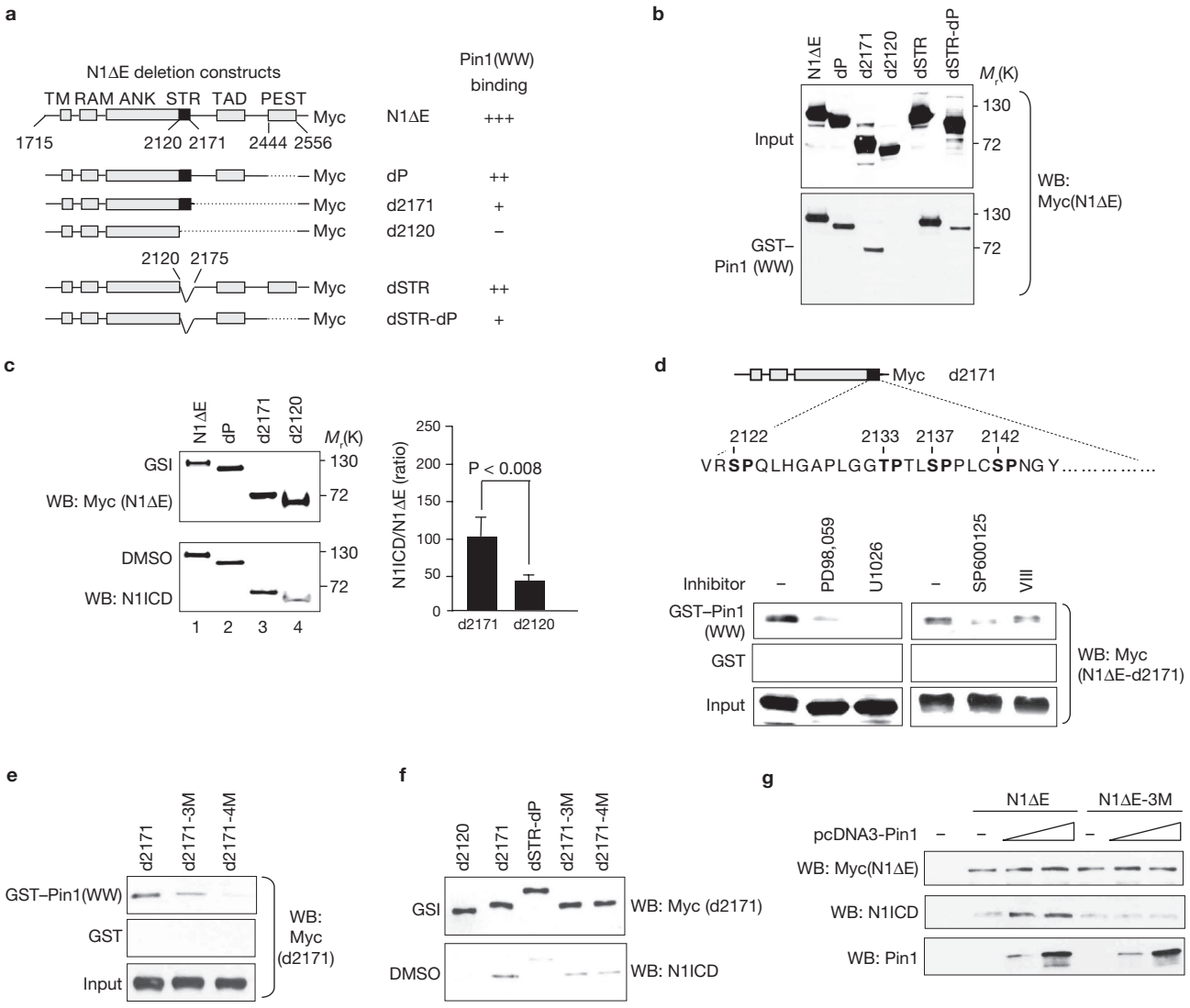

Figure 4 Pin1 improves cleavage of Notch1 by binding to the STR region. (**a**) Schematic representation of pBabe–N1ΔE–Myc deletion constructs used in experiments in **b**. TM, transmembrane; RAM, CSL interacting; ANK, ankyrin; STR, Ser-Thr-rich; TAD, transactivation; PEST, Pest domain. Numbering refers to Swissprot entry P46531. Interactions with Pin1 (**b**) are indicated next to the constructs (+++, strong; ++, intermediate; +,weak; – no binding). (**b**) Mapping of Pin1 binding domains of Notch1. Western blot analysis of GST–Pin1 (WW) or GST (data not shown) pulldown assay of indicated proteins is shown. (**c**) Impaired processing of N1ΔE proteins lacking STR. Cleavage of N1ΔE deletion mutants was analysed by western blotting after overexpression in SKBr-3 cells treated with either GSI (DAPT, 20 μM) or DMSO. Left upper panel shows uncleaved GSI-treated inputs and lower panel shows cleavage products recognized by the anti-Val 1744 antibody (N1ICD). Right panel shows the ratio (percentage) of N1ICD (cleaved) to the corresponding uncleaved form, calculated as in Fig. 2. (**d**) Interaction of Pin1 with the STR region is impaired by MAP/SAPK inhibitors. Schematic representation of the STR domain showing Ser/Thr-Pro motifs (bold). pCDNA3-d2171-Myc was tested for Pin1 binding as in **b**, either in absence (–) or presence of MAPK (left) or JNK (right) inhibitors. (**e**) Mutation of Ser/Thr-Pro motifs in the STR region impairs binding to Pin1. Constructs pcDNA3-d2171-Myc, pcDNA3-d2171-3M–Myc and pcDNA3-d2171-4M–Myc were overexpressed in HEK293T cells and tested for Pin1 binding as in **b**. (**f**) Mutation of Ser/Thr-Pro motifs in STR (d2171-3M and d2171-4M) impairs processing by γ-secretase. The indicated point-mutants of N1ΔE-d2171 were overexpressed in SKBr-3 cells and their processing analysed as in **c**. (**g**) Substitution of the Ser/Thr-Pro sites Ser 2122, Thr 2133 and Ser 2137 to Ala (N1ΔE-3M) hampers the Pin1-dependent increase in processing by γ-secretase. Comparable amounts of pcDNA3-N1ΔE–Myc or pcDNA3-N1ΔE-3M–Myc were overexpressed in *Pin1*$^{-/-}$ fibroblasts along with empty vector (–) or increasing amounts of Pin1-expressing vector (open triangles), and processing was analysed as in **c**. Complete scans of the western blots are shown in Supplementary Information, Fig. S6.

finding that in human breast cancers, elevated levels of Pin1 correlate with deregulated expression of activated Notch1 and HES-1, underscores the relevance of our observations for human carcinogenesis.

The increasing evidence that Notch signalling can drive the growth of a wide range of tumours, from leukaemia to breast cancer, has recently prompted intense study of the mechanisms underlying alteration of this pathway during carcinogenesis[2,5]. However, several crucial aspects remain obscure, particularly concerning the regulation of Notch1 processing and how its downstream effects contribute to the neoplastic phenotype. One crucial point in Notch activation entails proteolytic cleavage by γ-secretase, but several mechanisms that impinge on this step are still unclear[4,36–39]. Shedding of the extracellular domain of Notch receptors is required for γ-secretase cleavage to occur[3,36,38,39], but our data show that the intracellular STR region of Notch1 may also be required for efficient

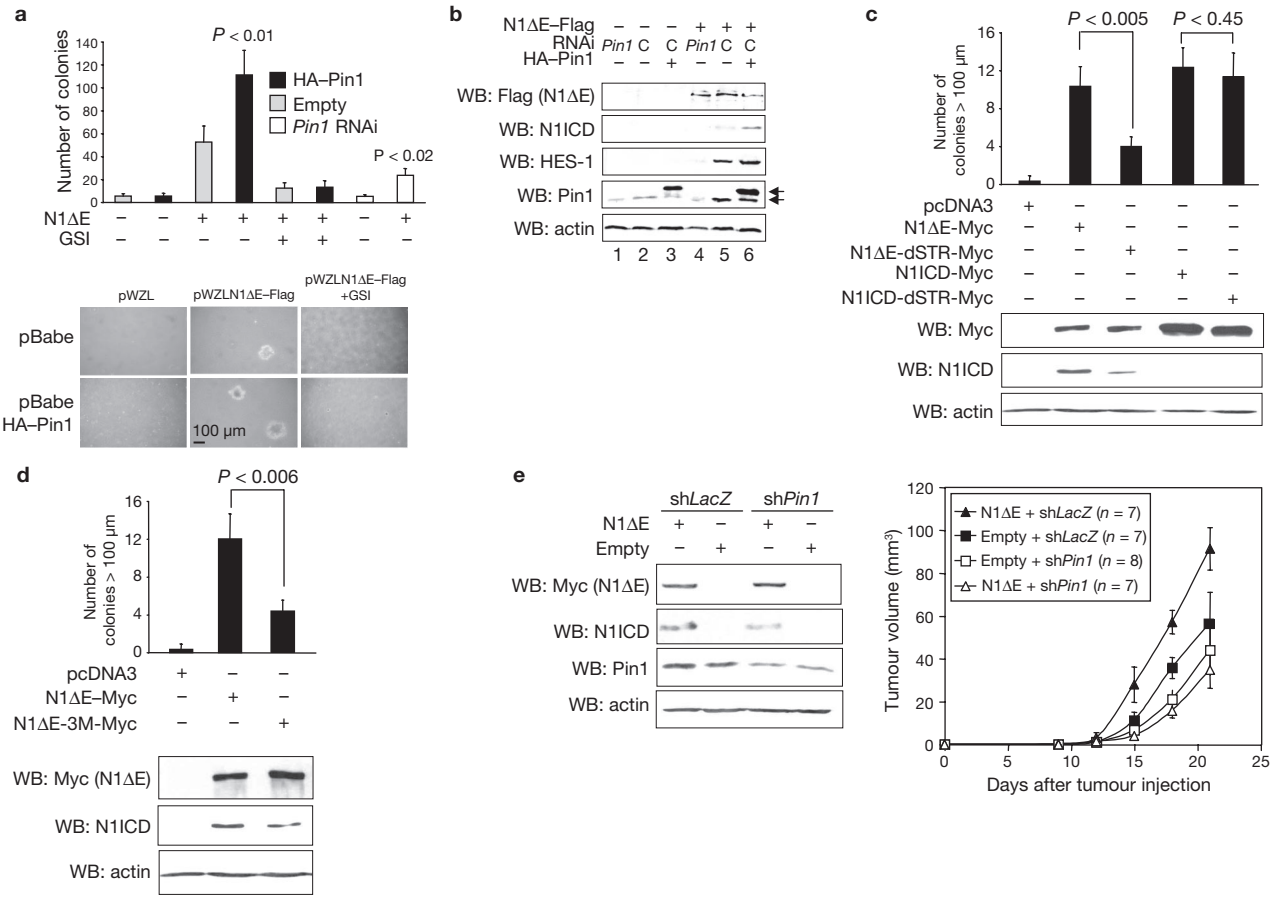

Figure 5 Pin1 affects human Notch1 tumorigenic activity. (**a**) Notch1 transforming activity is modulated by Pin1. Histograms show the number of colonies formed in soft agar of normal MCF-10A breast epithelial cells, transduced with retroviruses encoding N1ΔE–Flag along with empty vector or vectors for HA–Pin1, *Pin1* or control shRNA (control shRNA data not shown), with or without GSI (DAPT, 20 μM) treatment. Colonies were counted after 3 weeks. Histograms represent mean ± s.d. of three independent experiments (*P* values for the observed difference between N1ΔE and N1ΔE with either HA–Pin1 or *Pin1* RNAi are shown). Representative phase-contrast images of soft agar colonies of the indicated clones are shown in the lower panel. (**b**) Protein lysates were analysed by western blotting. Arrows indicate endogenous (lower) and overexpressed (upper) Pin1. Complete scans of the western blots are shown in Supplementary Information, Fig. S6. (**c**) Deletion of the STR region in membrane-tethered N1ΔE, but not in nuclear N1ICD, reduces Notch1 transforming activity. The upper panel shows the number of colonies, on soft agar, exceeding 100 μm in diameter, of MDA-MB-231 cells stably expressing empty vector, N1ΔE–Myc, N1ΔE-dSTR–Myc, N1ICD–Myc or N1ICD-dSTR–Myc. Histograms represent mean± s.d. of three independent experiments. Lower panel shows western blot analysis of protein lysates. Overexpressed N1ICD was not recognized by the anti-N1ICD (Val 1744) antibody because it does not contain this epitope. (**d**) Mutation of Ser 2122, Thr 2133 and Ser 2137 in the STR region (N1ΔE-3M) is sufficient to impair processing efficiency and transformation activity of Notch1. MDA-MB-231 cells stably expressing empty vector, N1ΔE–Myc or N1ΔE-3M–Myc were grown in soft agar. Colonies were counted and protein lysates analysed as in **c**. (**e**) Knockdown of endogenous *Pin1* reduces Notch1-induced tumour growth in xenografted nu/nu mice. The left panel shows a western blot of MDA-MB-231 cells, stably expressing empty vector or N1ΔE–Myc along with *Pin1* or *LacZ* shRNA (sh*Pin1* and sh*LacZ*), used for xenograft in nude mice. The right panel shows *in vivo* tumour growth curves of the cells shown in the left panel after inoculation as subcutaneous xenografts in immunodeficient mice. Data are mean ± s.e.m of the tumour volumes (*P* < 0.0006, N1ΔE+shLacZ versus N1ΔE+sh*Pin1*; Student's *t*-test; *n* indicates injected mice).

processing. This region is conserved between Notch1 and Notch2 and has been shown to be phosphorylated in response to cytokine-induced differentiation of 32D cells[31].

Recent studies suggest that although Notch1 and presenilin-1 are already associated before cleavage, proficient recognition of and access to the active site of the γ-secretase complex occurs only after receptor activation[38,40,41]. In our experiments, presenilin-1 levels and association with endogenous Notch1 or constitutively activated N1ΔE did not change with modulation of Pin1 levels (Supplementary Information, Fig. S2b and data not shown). Therefore our results, obtained by mimicking Notch1 activation by EDTA treatment or ectopic expression of constitutively cleaved N1ΔE, suggest that Pin1, on binding to crucial Ser/Thr-Pro sites within STR after phosphorylation, produces a conformational change in Notch1 that could favour processing by γ-secretase. Indeed, we have shown that deletion of this region, or mutation of the crucial phosphorylation and Pin1 binding sites, impairs the constitutive processing of N1ΔE. Notably, phosphorylation-dependent prolyl-isomerization by Pin1 has been related to proteolytic processing of APP[20,21], another γ-secretase substrate, supporting our hypothesis that conformational changes of the cytosolic domain of type I transmembrane proteins could be important for regulated intramembrane proteolysis. To prevent sporadic activation in the absence of ligand-binding, Notch1 cleavage must be tightly regulated at several levels, including endocytic trafficking and degradation mediated by Numb

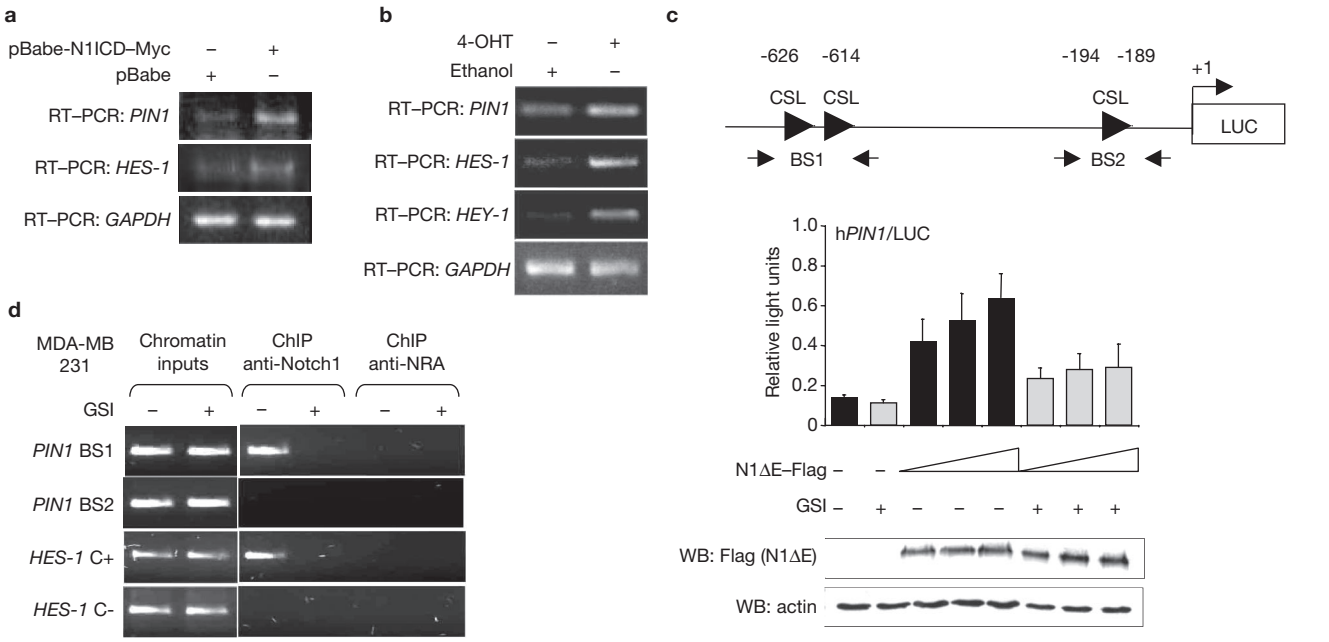

Figure 6 Pin1 is a transcriptional target of Notch1. (**a**) N1ICD enhances *Pin1* mRNA levels. RT–PCR analysis of the indicated genes from MCF-7 cells stably transfected with an empty or N1ICD expressing vector. (**b**) N1ICD activation enhances *Pin1* mRNA levels. RT–PCR analysis of *PIN1*, *HES-1* and *HEY-1* in H1299 cells stably expressing ER-N1ICD after 24 h of mock (ethanol) or 4-OH-tamoxifen (OHT) induction. Human *GAPDH* has been included for normalization (**a**, **b**). (**c**) Notch1 activates the human *PIN1* promoter. The upper panel shows a schematic representation of the human *PIN1* promoter (genomic sequence from –713 to +53 with respect to the ATG) depicting CSL binding sites (with numbering) and indicating the primer sets used for ChIP analysis in **d**. The depicted genomic region of the human *PIN1* promoter was PCR amplified and cloned into pGL3/LUC, as described in detail in the Supplementary Information. The lower panel shows reporter assays of pGL3hPin1/LUC on N1ΔE–Flag expression in SKBr-3 cells in presence (grey columns) or absence (black columns) of GSI. Histograms represent mean ± s.d. of three independent experiments. Cell lysates were analysed by western blotting. (**d**) Endogenous Notch1 associates with the human *PIN1* promoter. Binding of endogenous N1ICD to the human *PIN1* promoter, analysed by ChIP analysis in MDA-MB-231 cells, treated either with DMSO (–) or GSI (+), is shown. Semi-quantitative PCR analysis of *PIN1* promoter (sequences BS1 and BS2) or *HES-1* promoter as a positive control (C+) or *HES*-1 intron[50] as a negative control (C) were performed with anti-Notch1 or unrelated (anti-NRA)antibody in chromatin immunoprecipitates.

and several E3-ligases[37,42]. It is possible therefore that, in addition to a direct effect on Notch1 cleavage, prolyl-isomerization by Pin1 could affect processing by altering the ability of Notch1 to interact with these factors[43]. Considering the plethora of Pin1 substrates, however, we cannot exclude that Pin1 could also affect the activity of these factors.

Notch1 processing was shown to be increased in Ras-transformed cells[8]. Our observation that Pin1 binding to Notch1 involves MAPK/SAPKs, coupled with evidence that Pin1 expression is induced by Ras[22], suggests a role of Pin1 in the activation of Notch1 by oncogenic stress.

Pin1 regulates transcriptional activity of several factors[12,13]; thus it may contribute to potentiating Notch1 functions by modulating its nuclear activity. Recently, N1ICD was shown to be upregulated in thymic lymphocytes from *p53*;*Pin1* double-knockout mice[44]. The authors showed that Pin1 interacts with N1ICD and claimed that Pin1 could negatively affect N1ICD stability. This apparent discrepancy with our data may be explained by the *p53* knockout context, where presenilin-1 is known to be upregulated and enhance Notch1 activation[45], and this could be exacerbated by loss of Pin1 by other, yet unknown, mechanisms. Indeed loss of Pin1 alone in thymic lymphocytes bearing endogenous p53 does not cause upregulation of N1ICD levels[44] or of presenilin-1, in agreement with our observations (Supplementary Information, Fig. S2b).

Notch1-dependent cellular processes involve induction of a repertoire of target genes[2,11]. We have now established that Pin1 is a direct transcriptional target of Notch1. This result is particularly relevant because it suggests that Pin1 and Notch1, by interacting at multiple levels, establish an important molecular circuitry. By upregulating Pin1, Notch1 enhances its own processing and activation. In addition, Pin1 may affect N1ICD activity and it could also directly affect some Notch1 transcriptional targets, such as cyclin D1 and NF-κB[17,19], further amplifying the Notch1 signal.

The relevance of this molecular circuitry to human carcinogenesis is clear as Pin1 and Notch1 cooperate in transformation assays and also in tumorigenesis *in vivo*. Furthermore, the strong correlation between levels of Pin1, Notch1 and HES-1, shown in human tumours, could have important implications for therapeutic intervention. Indeed, we have clearly shown that inhibition of Pin1 function together with GSI administration affects the growth of breast cancer cells with activated Notch1 signalling. Targeting γ-secretase to block Notch1 signalling is considered a promising strategy for therapy of human cancers, particularly breast tumours[5,11]. However GSIs, although effective *in vitro*, have a toxic effect due to their action on normal stem cells[5,11]. On the basis of our results, it is tempting to predict that in tumours with deregulated expression of both Notch1 and Pin1, a lower dose of GSI could provide a better response if administered in combination with Pin1 inhibitors. □

METHODS

Cell lines and treatments. SKBr-3, MDA-MB-468, MDA-MB-231 and MCF-7 are human breast carcinoma cells (MCF-7 were purchased from IZS). The nature of MDA-MB-435, mis-identified as breast cancer cell line for several decades, has

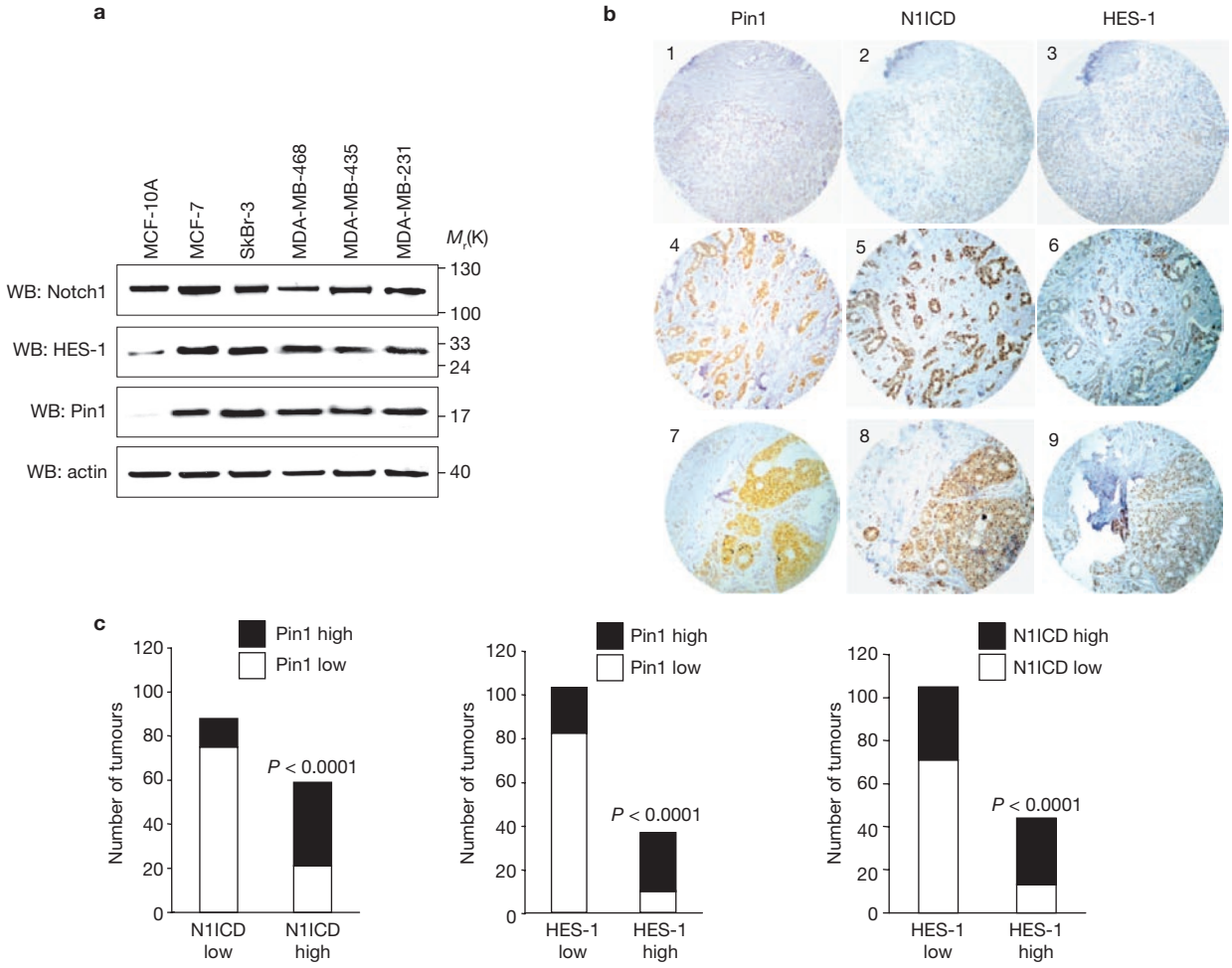

Figure 7 Expression of Pin1, Notch1 and HES-1 in breast cancer cell lines and in serial sections of breast carcinoma samples. (**a**) Western blot analysis of a human immortalized breast cell line (MCF-10A), four breast cancer cell lines (MCF-7, SKBr-3, MDA-MB-468, MDA-MB-231) and the MDA-MB-435 cell line (see Methods) is shown for Notch1, Pin1 and HES-1, normalized by actin levels. (**b**) Representative samples showing results of immunohistochemical analysis of breast tissue microarrays performed with the indicated antibodies on adjacent sections of the same array. Shown are examples of breast carcinoma negative for all three proteins (1–3) and examples of moderate to strong expression for N1ICD, Pin1 and HES-1 on two different breast cancer samples (4–9). Original magnification ×20. (**c**) Graphs showing correlation between Pin1, HES-1 and N1ICD expression levels in breast cancer. Bars represent the number of tumours in low and high expression groups of N1ICD, Pin1 and HES-1; *P* values of observed differences, according to Pearson's chi-square, are indicated.

recently been disputed[46,47]. MCF-10A are human normal immortalized epithelial breast cells, HEK 293T is a human embryonic kidney cell line with SV40 large T, H1299 is a human lung carcinoma cell line. Immortalized *Pin1*$^{-/-}$ fibroblasts were obtained by spontaneous immortalization from MEFs of C57BL6/129Sv mixed background[30]. All cells, except for H1299 and MCF-10A cells, were cultured in DMEM (BioWhittaker) supplemented with 10% fetal bovine serum (Gibco) and penicillin/streptomycin. H1299 cells were grown in RPMI, and MCF-10A cells were maintained in DMEM:F12 Ham's (1:2; Sigma), supplemented with 5% horse serum (Gibco), insulin (10 μg ml^{-1}; Sigma), hydrocortisone (0.5 μg ml^{-1}) and EGF (20 ng ml^{-1}; Peprotech). Transient transfections and luciferase assays were performed using standard procedures[14,16]. For creation of stable clones, a selection corresponding to the expressed vectors was applied for 2 weeks to transfected or infected cells at concentrations of 50 μg ml^{-1} for hygromycin, 2 μg ml^{-1} for puromycin and 0.5 mg ml^{-1} for neomycin. The γ-secretase inhibitor DAPT (Sigma) and Pin1 inhibitor PiB (Calbiochem) were dissolved in DMSO and used at final concentrations of 20 and 0.5 μM respectively, except in growth curves where the concentrations are indicated in the figures. For EDTA treatment, cells were washed twice in PBS, then PBS or PBS containing either EDTA (5 mM) or EDTA (5 mM) plus GSI was added for 15 min, followed by a 15-min chase in culture medium, washed and collected, as described previously[29]. For processing experiments with N1ΔE deletion constructs, transfected cells were split into two parts and treated with either GSI or DMSO. Kinase inhibitors U0126, PD98,059 (Sigma), SP600125 (Biosource) and VIII (Calbiochem) were solubilized in DMSO and used at a final concentration of 10 μM for 30 min to 1 h. For MDA-MB-231 growth curves, 75,000 or 100,000 cells, with the indicated inhibitors, were seeded into 6-well plates at day 0 in duplicate for each planned time-point. Every second day, cells of the corresponding time-point were trypsinized and counted. Cells from the last time-points were collected after counting and lysed for western blot analysis.

Phosphatase treatment, *in vitro* binding, immunoprecipitation, western blot and far western. Pin1 *in vitro* binding assays and co-immunoprecipitation, as well as phosphatase treatment were performed using standard procedures[14,16]. Briefly, for GST pulldown analysis, the lysis buffer was supplemented with phosphatase inhibitors (1 mM sodium orthovanadate, 5 mM NaF) and protease inhibitors (1 mM phenylmethylsulphonylfluoride (PMSF) and 10 μg ml^{-1} each of chymostatin, leupeptin, antipain, pepstatin,). In the case of phosphatase treatment, phosphatase inhibitors were omitted, λ-phosphatase (400 U ml^{-1}) was added to cell extracts and the reaction continued for 2 h at 30°C, according to the manufacturer's instructions (New England Biolabs) before GST pulldown or immunoprecipitation.

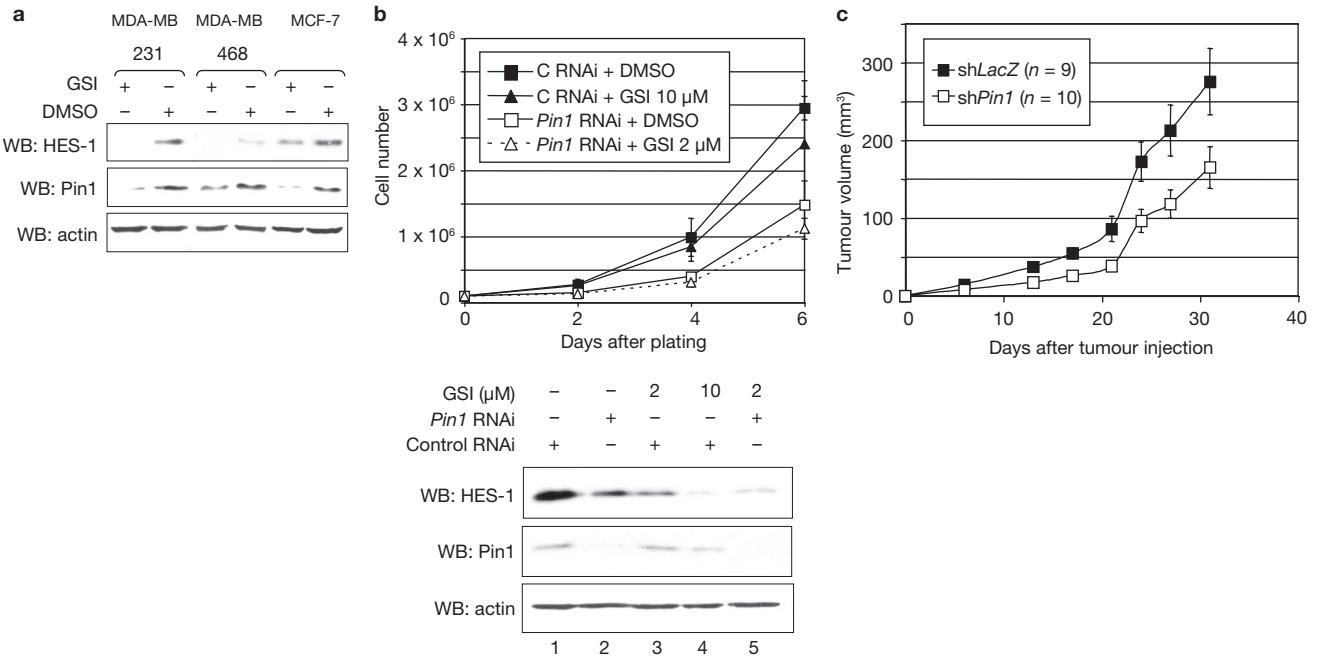

Figure 8 Inhibition of Pin1 sensitizes human breast cancer cell lines to GSI treatment. (**a**) Treatment of cells with GSI downregulates the levels of Notch1 targets Pin1 and HES-1. Western blot analysis of breast cancer cell lines treated for 10 days with vehicle (DMSO) or GSI (DAPT, 10 μM). (**b**) Effect of Pin1 ablation on sensitivity of breast cancer cell growth to GSI. The upper panel shows growth curves for MDA-MB-231 breast cancer cells treated with GSI (DAPT) at the indicated concentrations in *Pin1*-ablated (open symbols) or control RNAi cells (RISC-free, black symbols). Cells were counted every two days for 6 days after plating. Data are mean ± s.d. of three independent experiments, each performed in duplicate. $P < 10^{-4}$, DMSO versus GSI; $P < 0.0003$, DMSO + control RNAi versus DMSO + *Pin1* RNAi; $P < 0.006$, 10 μM GSI + control RNAi versus 2 μM GSI + *Pin1* RNAi (Student's *t*-test). The lower panel shows western blot analysis of Notch1 target HES-1 following GSI treatment with or without *Pin1* knockdown. Complete scans of the western blots are shown in Supplementary Information, Fig. S6. (**c**) *In vivo* tumour growth curves for MDA-MB-231 cells expressing sh*LacZ* or sh*Pin1* following orthotopic injection into the mammary fat pad of immunodeficient mice. Data are mean ± s.e.m of the tumour volumes of *Pin1*-ablated (open symbol) or control cells (black symbol). $P < 0.03$, sh*LacZ* versus sh*Pin1* (Student's *t*-test; *n* indicates number of injected mice).

For Pin1 immunoprecipitation assays, cells were collected in PBS pH 8.3 buffer (PBS pH 8.3, 0.1% Tween-20) and lysed by passing through a 26 G needle. For Notch1 immunoprecipitations, cells were collected in GST pulldown buffer (150 mM NaCl, 50 mM Tris/HCl pH 7.5, 10% glycerol, 0.1% nonidet P-40). Cell lysates were cleared with proteinA Sepharose, with rocking for 30 min, then protein A/G Sepharose (GE Healthcare) crosslinked antibodies, pre-cleared with BSA (10 mg ml^{-1}), were added. Binding reactions were left for a minimum of 4 h to overnight, with rocking at 4°C. Beads were then washed, and bound proteins were loaded and separated in SDS–PAGE, followed by western blotting on nitrocellulose membranes (Scleicher & Schuell).

Purified GST–Pin1 protein for far-western analysis was obtained by immobilization, after production in bacteria, on glutathione sepharose 4B beads (GE Healthcare) followed by elutions using reduced GSH as a competitor in Tris/HCl (100 mM, pH 8) and NaCl (100 mM). The eluted protein was subsequently purified by dialysis.

For far-western blot analysis, proteins were immunoprecipitated with the indicated antibody, resolved by SDS–PAGE and blotted onto nitrocellulose membrane. Blocking was performed for 1 h at 4°C in PBS containing 10% not-fat dry milk. Blots were then incubated with GST–Pin1 protein (1 μg ml^{-1}) in blocking buffer for 1 h. Membranes were washed 4 times in PBS, 0.2% Tween-20. Subsequently, recognition by standard western blotting was performed. Densitometric values of protein levels in western blot analyses were obtained by Image J software.

***In vivo* tumour growth experiments.** Five-to-seven week-old female athymic nude mice were purchased from Harlan Italy, and housed in a specific pathogen-free (SPF) animal facility. Procedures involving animals and their care conformed to institutional guidelines that comply with national and international laws and policies. For xenograft studies of breast cancer, MDA-MB-231 cell clones were injected subcutaneously or into the mammary fat pad, and tumour growth at the injection site was monitored by repeated caliper measurements. Tumour volume was calculated using the formula: tumour volume (mm^3) = $D \times d^2/2$, where D and d are the longest and the shortest diameters, respectively. The *in vivo* tumour growth experiments were conducted according to the UK Coordinating Committee on Cancer Research (UKCCCR) guidelines for the welfare of animals in experimental neoplasia[48]. During *in vivo* experiments, animals in all experimental groups were examined daily for a decrease in physical activity and other signs of disease; severely ill animals were euthanized by CO_2 asphyxiation.

Tissue microarray (TMA) construction and immunohistochemical analysis (IHC). Formalin-fixed and paraffin-embedded tissue specimens for TMA construction were obtained from Istituto Europeo di Oncologia (Milan, Italy). TMAs were prepared as described previously[49]. Briefly, two representative tumour areas (diameter 0.6 mm) from each sample, identified previously on sections stained with haematoxylin and eosin, were removed from the donor block and deposited on the recipient block using a custom-built precision instrument (Tissue Arrayer, Beecher Instruments). Serial sections (3 μm) of the resulting recipient block were cut, mounted on glass slides and processed for immunohistochemistry with rabbit polyclonal anti-Pin1 (1:200, Calbiochem), rabbit polyclonal anti-N1ICD (1:750, Chemicon), and mouse monoclonal anti-HES-1 (clone NM1, 1:500, MBL) antibodies. A tyramide signal-amplification labelling kit (TSA kit no. 21, cat no. T20931, Invitrogen) was used for signal enhancement of anti-N1ICD and anti-HES-1 immunohistochemical stains. Arbitrary cut-offs for definition of low and high protein expression levels used for statistical analysis were established according to both intensity of staining (from 0–3) and percentage of stained cells (from 0–100%) in the tumour nuclei. A semi-quantitative score from 0–300 was obtained. For each gene, cases showing a score below the mean were classified as 'low expression' and cases above the mean as 'high expression'. Statistically significant differences were assessed according to Pearson's chi-square.

Statistical analyses. For transfection, processing, cell and tumour growth experiments *P*-values were obtained by applying a one-tailed, type 2 *t*-test (assuming equal variances) using Microsoft Excel. For TMA analysis *P*-values were obtained from Pearson's chi-square test.

Note: Supplementary Information is available on the Nature Cell Biology website.

ACKNOWLEDGEMENTS

We thank LNCIB colleagues, F. Mantovani , L. Collavin and S. Piccolo for critical reading of the manuscript; R. Poddighe for technical support, and M. Stebel and C. Degrassi of the C.S.P.A., University of Trieste. We are grateful to M. Donzelli for generation of the pcDNA3$^{N1\Delta E}$–Flag construct, to T. Sudo for the anti-HES-1 antibody, A. Israel for pGL2-HES-1/LUC, T. Uchida for providing *Pin1* knockout mice and to ICGEB for access to their facilities. This work was supported by grants from Associazione Italiana per la Ricerca sul Cancro (AIRC), from Italian University and Research Ministerium (Cofin MIUR), from Friuli-Venezia-Giulia (regional grant), from Association for International Cancer Research (AICR, UK) to G.D.S., and from R01 CA-83736-07 to A.C, AIRC and Fondazione Giancarla Vollaro to S.P. and to Fondazione Monzino and AIRC to P.P.D.F.; M.N. is a FIRC fellow (Fondazione Italiana per la Ricerca sul Cancro). This paper is dedicated to the memory of Stefano Ferrari.

AUTHOR CONTRIBUTIONS

A.R., L.T., A.S. and M.N. performed biochemical and cell biology experiments; P.N. performed analysis and evaluation of TMA under the supervision of S.P. and P.P.D.F; A.R. performed part of the *in vivo* experiments; F.K. and A.C. provided essential reagents and assisted with scientific support; G.D.S. was responsible for the overall project.

COMPETING FINANCIAL INTERESTS

The authors declare no competing financial interests.

Published online at http://www.nature.com/naturecellbiology/
Reprints and permissions information is available online at http://npg.nature.com/reprintsandpermissions/

1. Artavanis-Tsakonas, S., Rand, M. D. & Lake, R. J. Notch signaling: cell fate control and signal integration in development. *Science* **284,** 770–776 (1999).
2. Radtke, F. & Raj, K. The role of Notch in tumorigenesis: oncogene or tumour suppressor? *Nature Rev. Cancer* **3,** 756–767 (2003).
3. De Strooper, B. *et al.* A presenilin-1-dependent γ-secretase-like protease mediates release of Notch intracellular domain. *Nature* **398,** 518–522 (1999).
4. Bray, S. J. Notch signalling: a simple pathway becomes complex. *Nature Rev. Mol. Cell Biol.* **7,** 678–689 (2006).
5. Garber, K. Notch emerges as new cancer drug target. *J. Natl Cancer Inst.* **99,** 1284–1285 (2007).
6. Ayyanan, A. *et al.* Increased Wnt signaling triggers oncogenic conversion of human breast epithelial cells by a Notch-dependent mechanism. *Proc. Natl Acad. Sci. USA* **103,** 3799–3804 (2006).
7. Pece, S. *et al.* Loss of negative regulation by Numb over Notch is relevant to human breast carcinogenesis. *J. Cell Biol.* **167,** 215–221 (2004).
8. Weijzen, S. *et al.* Activation of Notch-1 signaling maintains the neoplastic phenotype in human Ras-transformed cells. *Nature Med.* **8,** 979–986 (2002).
9. Kiaris, H. *et al.* Modulation of notch signaling elicits signature tumors and inhibits hras1-induced oncogenesis in the mouse mammary epithelium. *Am. J. Pathol.* **165,** 695–705 (2004).
10. Stylianou, S., Clarke, R. B. & Brennan, K. Aberrant activation of notch signaling in human breast cancer. *Cancer Res.* **66,** 1517–1525 (2006).
11. Miele, L., Golde, T. & Osborne, B. Notch signaling in cancer. *Curr. Mol. Med.* **6,** 905–918 (2006).
12. Yeh, E. S. & Means, A. R. PIN1, the cell cycle and cancer. *Nature Rev. Cancer* **7,** 381–388 (2007).
13. Lu, K. P. & Zhou, X. Z. The prolyl isomerase PIN1: a pivotal new twist in phosphorylation signalling and disease. *Nature Rev. Mol. Cell Biol.* **8,** 904–916 (2007).
14. Zacchi, P. *et al.* The prolyl isomerase Pin1 reveals a mechanism to control p53 functions after genotoxic insults. *Nature* **419,** 853–857 (2002).
15. Mantovani, F. *et al.* The prolyl isomerase Pin1 orchestrates p53 acetylation and dissociation from the apoptosis inhibitor iASPP. *Nature Struct. Mol. Biol.* **14,** 912–920 (2007).
16. Mantovani, F. *et al.* Pin1 links the activities of c-Abl and p300 in regulating p73 function. *Mol. Cell* **14,** 625–636 (2004).
17. Liou, Y. C. *et al.* Loss of Pin1 function in the mouse causes phenotypes resembling *cyclin D1*-null phenotypes. *Proc. Natl Acad. Sci. USA* **99,** 1335–1340 (2002).
18. Ryo, A., Nakamura, M., Wulf, G., Liou, Y. C. & Lu, K. P. Pin1 regulates turnover and subcellular localization of β-catenin by inhibiting its interaction with APC. *Nature Cell Biol.* **3,** 793–801 (2001).
19. Ryo, A. *et al.* Regulation of NF-κB signaling by Pin1-dependent prolyl isomerization and ubiquitin-mediated proteolysis of p65/RelA. *Mol. Cell* **12,** 1413–1426 (2003).
20. Pastorino, L. *et al.* The prolyl isomerase Pin1 regulates amyloid precursor protein processing and amyloid-β production. *Nature* **440,** 528–534 (2006).
21. Akiyama, H., Shin, R. W., Uchida, C., Kitamoto, T. & Uchida, T. Pin1 promotes production of Alzheimer's amyloid β from β-cleaved amyloid precursor protein. *Biochem. Biophys. Res. Commun.* **336,** 521–529 (2005).
22. Wulf, G., Garg, P., Liou, Y. C., Iglehart, D. & Lu, K. P. Modeling breast cancer *in vivo* and *ex vivo* reveals an essential role of Pin1 in tumorigenesis. EMBO *J.* **23,** 3397–3407 (2004).
23. Bao, L. *et al.* Prevalent overexpression of prolyl isomerase Pin1 in human cancers. *Am. J. Pathol.* **164,** 1727–1737 (2004).
24. Wulf, G., Ryo, A., Liou, Y. C. & Lu, K. P. The prolyl isomerase Pin1 in breast development and cancer. *Breast Cancer Res.* **5,** 76–82 (2003).
25. Jarriault, S. *et al.* Signalling downstream of activated mammalian Notch. *Nature* **377,** 355–358 (1995).
26. Schroeter, E. H., Kisslinger, J. A. & Kopan, R. Notch-1 signalling requires ligand-induced proteolytic release of intracellular domain. *Nature* **393,** 382–386 (1998).
27. Zhou, X. Z. *et al.* Pin1-dependent prolyl isomerization regulates dephosphorylation of Cdc25C and tau proteins. *Mol.* **6,** 873–883 (2000).
28. Uchida, T. *et al.* Pin1 and Par14 pe *Cell* ptidyl prolyl isomerase inhibitors block cell proliferation. *Chem. Biol.* **10,** 15–24 (2003).
29. Rand, M. D. *et al.* Calcium depletion dissociates and activates heterodimeric notch receptors. *Mol. Cell Biol.* **20,** 1825–1835 (2000).
30. Fujimori, F., Takahashi, K., Uchida, C. & Uchida, T. Mice lacking Pin1 develop normally, but are defective in entering cell cycle from G.(0) arrest. *Biochem. Biophys. Res. Commun.* **265,** 658–663 (1999).
31. Ingles-Esteve, J., Espinosa, L., Milner, L. A., Caelles, C. & Bigas, A. Phosphorylation of Ser2078 modulates the Notch2 function in 32D cell differentiation. *J. Biol. Chem.* **276,** 44873–44880 (2001).
32. Ronchini, C. & Capobianco, A. J. Notch(ic)-ER chimeras display hormone-dependent transformation, nuclear accumulation, phosphorylation and CBF1 activation. *Oncogene* **19,** 3914–3924 (2000).
33. Maier, M. M. & Gessler, M. Comparative analysis of the human and mouse Hey1 promoter: Hey genes are new Notch target genes. *Biochem. Biophys. Res. Commun.* **275,** 652–660 (2000).
34. Osipo, C. *et al.* ErbB-2 inhibition activates Notch-1 and sensitizes breast cancer cells to a gamma-secretase inhibitor. *Oncogene* (2008).
35. O'Neill, C. F. *et al.* Notch2 signaling induces apoptosis and inhibits human MDA-MB-231 xenograft growth. *Am. J. Pathol.* **171,** 1023–1036 (2007).
36. Fortini, M. E. γ-secretase-mediated proteolysis in cell-surface-receptor signalling. *Nature Rev. Mol. Cell Biol.* **3,** 673–684 (2002).
37. Le Borgne, R., Bardin, A. & Schweisguth, F. The roles of receptor and ligand endocytosis in regulating Notch signaling. *Development* **132,** 1751–1762 (2005).
38. Wolfe, M. S. The γ-secretase complex: membrane-embedded proteolytic ensemble. *Biochemistry* **45,** 7931–7939 (2006).
39. Struhl, G. & Adachi, A. Requirements for presenilin-dependent cleavage of notch and other transmembrane proteins. *Mol. Cell* **6,** 625–636 (2000).
40. Ramdya, P., Skoch, J., Bacskai, B. J., Hyman, B. T. & Berezovska, O. Activated Notch1 associates with a presenilin-1/γ-secretase docking site. *J. Neurochem.* **87,** 843–850 (2003).
41. Schroeter, E. H. *et al.* A presenilin dimer at the core of the γ-secretase enzyme: insights from parallel analysis of Notch 1 and APP proteolysis. *Proc. Natl Acad. Sci. USA* **100,** 13075–13080 (2003).
42. Kanwar, R. & Fortini, M. E. Notch signaling: a different sort makes the cut. *Curr. Biol.* **14,** R1043–1045 (2004).
43. Chastagner, P., Israel, A. & Brou, C. AIP4/Itch regulates Notch receptor degradation in the absence of ligand. *PLoS ONE* **3,** e2735 (2008).
44. Takahashi, K. *et al.* Ablation of a peptidyl prolyl isomerase Pin1 from *p53*-null mice accelerated thymic hyperplasia by increasing the level of the intracellular form of Notch1. *Oncogene* **26,** 3835–3845 (2007).
45. Laws, A. M. & Osborne, B. A. p53 regulates thymic Notch1 activation. *Eur.* J. *Immunol.* **34,** 726–734 (2004).
46. Rae, J. M., Creighton, C. J., Meck, J M., Haddad, B. R. & Johnson, M. D. MDA-MB-435 cells are derived from M14 melanoma cells — a loss for breast cancer but a boon for melanoma research. *Breast Cancer Res. Treat.* **104,** 13–19 (2007).
47. Lacroix, M. MDA-MB-435 cells are from melanoma, not breast cancer. *Cancer Chemother Pharmacol* **63,** 567 (2008).
48. UKCCCR guidelines for the welfare of animals in experimental neoplasia. *Cancer Metastasis Rev.* **8,** 82–88 (1989).
49. Kononen, J. *et al.* Tissue microarrays for high-throughput molecular profiling of tumor specimens. *Nature Med.* **4,** 844–847 (1998).
50. Fryer, C. J., White, J. B. & Jones, K. A. Mastermind recruits CycC:CDK8 to phosphorylate the Notch ICD and coordinate activation with turnover. *Mol. Cell* **16,** 509–520 (2004).

nature cell biology

DOI: 10.1038/ncb1822

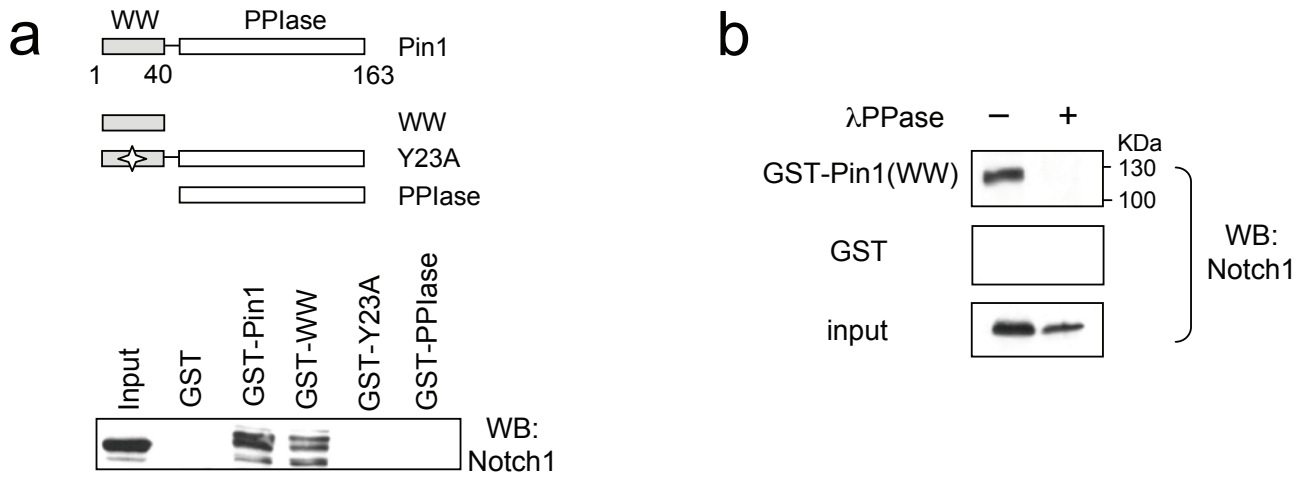

Figure S1 Characterization of the Pin1 and Notch1 interaction. **a)** Pin1 binding to Notch1 requires a functional WW domain and is phosphorylation-dependent. Schematic of full length GST-Pin1 and its truncation or point mutants. Y to A substitution in Y23A specifically abolishes the binding activity of the WW domain[1]. GST pull-down of lysates from SKBr-3 cells was performed incubating with GST, GST-Pin1 or the indicated GST-Pin1 mutants, followed by anti-Notch1 Western blot. **b)** Pin1 binding to Notch1 is phosphorylation-dependent. GST-Pin1 or GST pull-down experiments were performed using mock- or lambda phosphatase treated lysates from SKBr-3 cells, followed by anti-Notch1 Western blot.

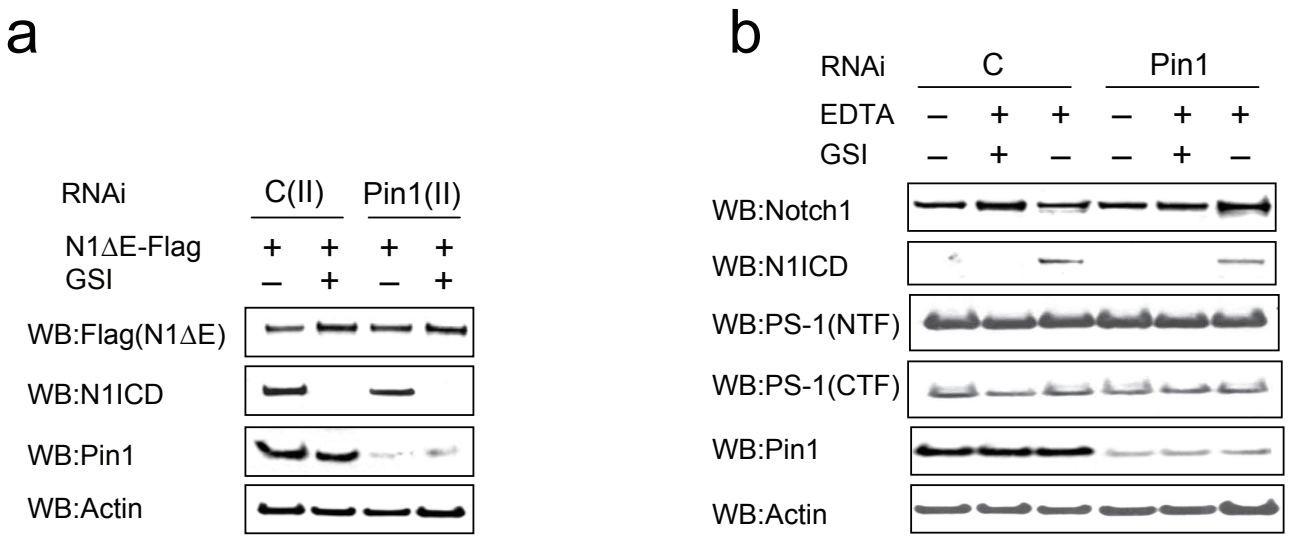

Figure S2 Specific Pin1 ablation affects Notch1 processing by γ-secretase. **a)** Ablation of Pin1 impairs N1ΔE constitutive processing. Western blot analysis of N1ΔE over-expressing SKBr-3 cells with Pin1(II) or control C(II) siRNA, is shown. **b)** Ablation of Pin1 impairs processing of endogenous Notch1. SKBr-3 cells transfected with Pin1 specific (Pin1) or control siRNA (C) were mock or EDTA treated as in Figure 3b, and indicated protein lysates were analysed by Western blot. Also included are Western blots against N- and C-terminal fragments of presenilin-1 (NTF and CTF, the core components of the gamma-secretase enzyme)[2].

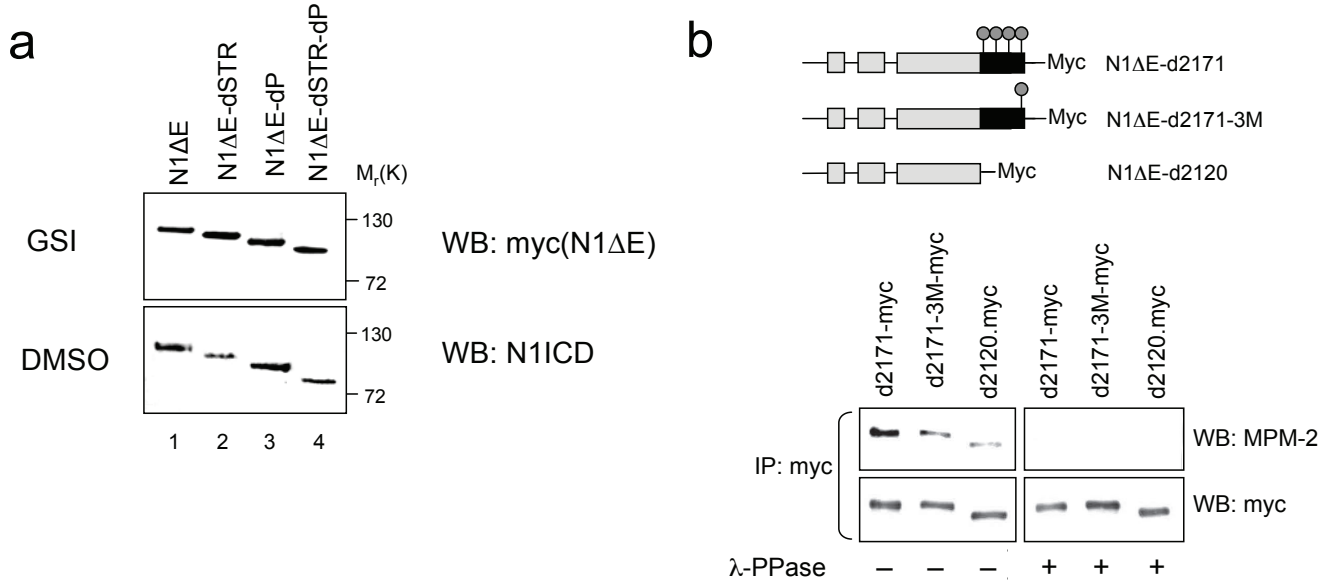

Figure S3 The STR region is important for the cleavage of Notch1 by γ-secretase. **a)** N1ΔE proteins lacking the STR region are impaired in cleavage by γ-secretase. Deletion constructs of myc-tagged N1ΔE (internal deletions of the STR region with or without the Pest domain) were transfected in SKBr-3 cells then split in two parts and treated with either GSI or DMSO to test for γ-secretase processing efficiency. Lysates were subjected to Western blot analysis. Upper panel shows Western blot of uncleaved, GSI treated proteins (input), while in the lower panel the cleavage products recognized by the Val 1744 antibody (N1ICD) are shown. **b)** Phosphorylation of S/T-P sites in the STR region. (Upper part) schematic of the tested proteins as shown in Fig. 4a, circles indicate putative phospho-S/T-P sites in the STR region. (Lower part) Western blot analysis with the phospho-S/T-P specific antibody MPM-2 of the indicated N1ΔE proteins. N1ΔE proteins over-expressed in HEK 293T in presence of GSI, were either left untreated (-) or λ–phosphatase treated (+), immunoprecipitated and recognized with the MPM-2 antibody; the membrane was stripped and recognized with an anti-myc antibody to show input levels. **c**) Kinase control experiments of Figure 4d. Western blot analyses of inputs of the GST pull-down of Fig. 4d were performed to control the effect of kinase inhibitors on phosphorylation and protein levels of classical endogenous kinase targets: (upper panel) MAPK targets Erk1/2 from untreated and MAPK inhibitor treated input lysates were analyzed by antibodies against phospho-Erk1/2 and total Erk1/2; (lower panel) the same as above for the JNK target c-jun. **d)** Mutation of Pin1 binding sites in the STR region renders cleavage insensitive to Pin1 over-expression. Western blot analysis of constitutive processing of N1ΔE-d2171-3M (left panel) or N1ΔE-d2171-4M (right panel) over-expressed in Pin1-/- fibroblasts along with empty vector (-) or increasing amounts of Pin1 expressing plasmid (open triangle). Anti-myc antibody recognizes uncleaved (GSI treated) inputs, anti-N1ICD blots show cleavage products (DMSO treated) and anti-Pin1 the levels of over-expressed Pin1.

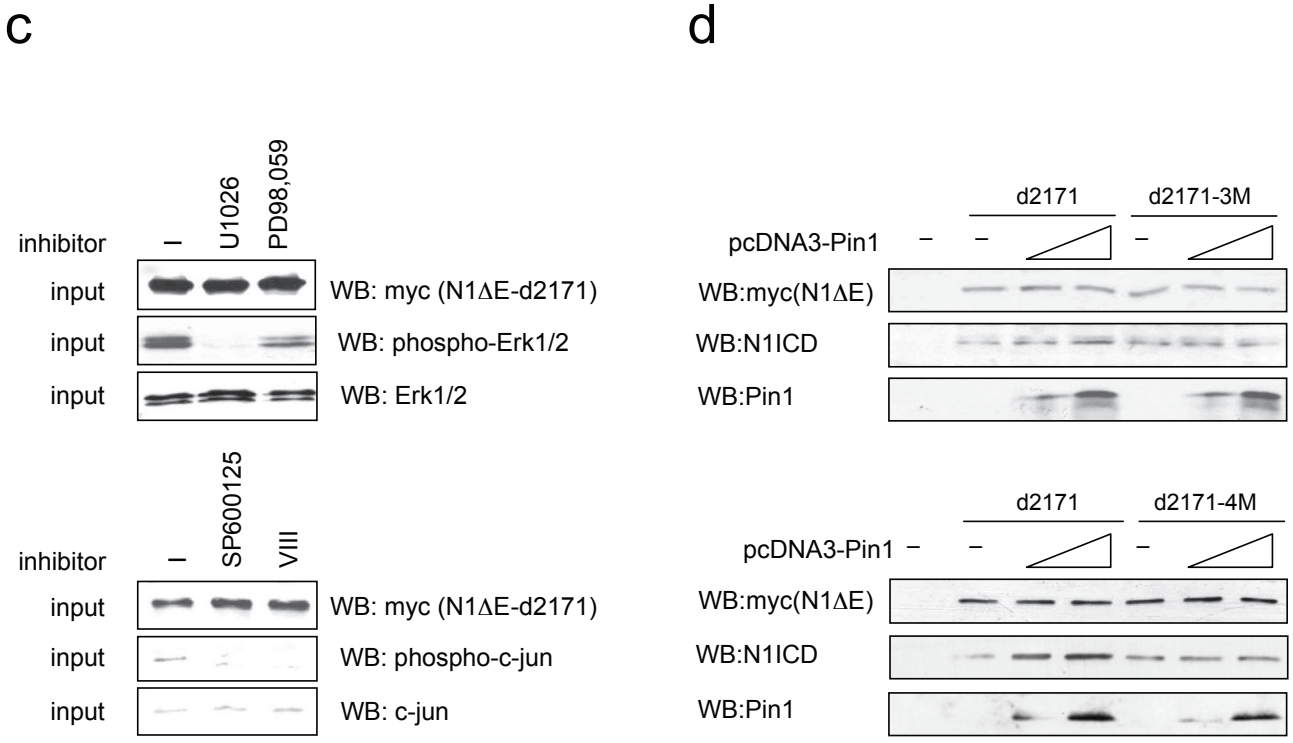

Figure S3 continued

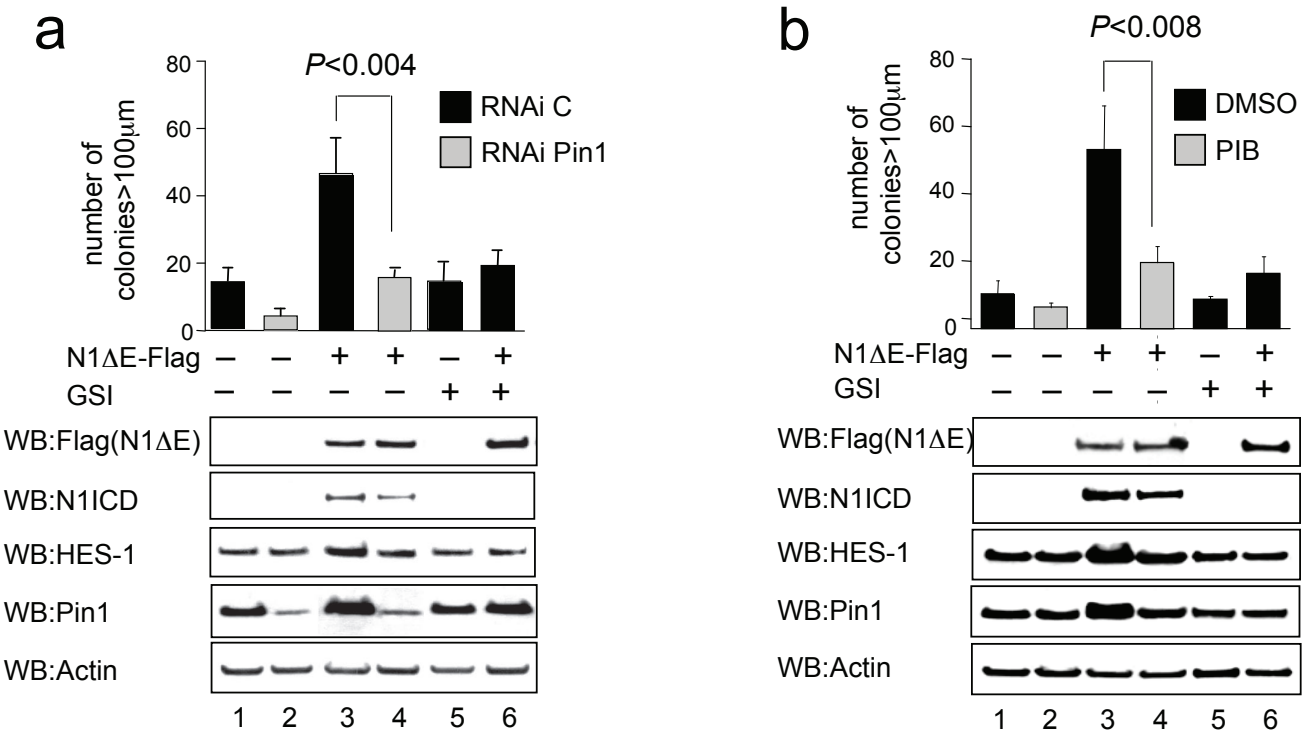

Figure S4 Pin1 affects Notch1 transforming activity in part by acting on the STR region. **a)** Knock-down of endogenous Pin1 reduces Notch1 transforming activity. Histograms show number of soft agar colonies of SKBr-3 cells stably expressing empty vector or Flag-N1ΔE along with control- (black bars) or Pin1-specific (grey bars) shRNA were grown in soft agar as described in Fig. 5. **b)** Inhibition of Pin1 catalytic activity with PiB reduces Notch1 transforming activity. Same as in a) but SKBr-3 cells, stably expressing vector or Flag-N1ΔE, were treated with DMSO (black bars) or small molecule inhibitor of Pin1 (PIB)(grey bars) or GSI as indicated. a) and b) Lower panels show Western analysis of protein lysates, *P* values were obtained as described in Fig.5. **c)** Effect of Pin1 knock-down on Notch1 transformation activty independent of processing. (upper panel) Histograms show number of soft agar colonies of MDA-MB-231 cells expressing empty vector (pCDNA3), N1ΔE-myc or N1ΔE-3M-myc along with control- (black bars) or Pin1-specific (grey bars) shRNA (Lower panel). Western blot analysis of protein lysates are shown below, *P* values were obtained as described in Fig.5.

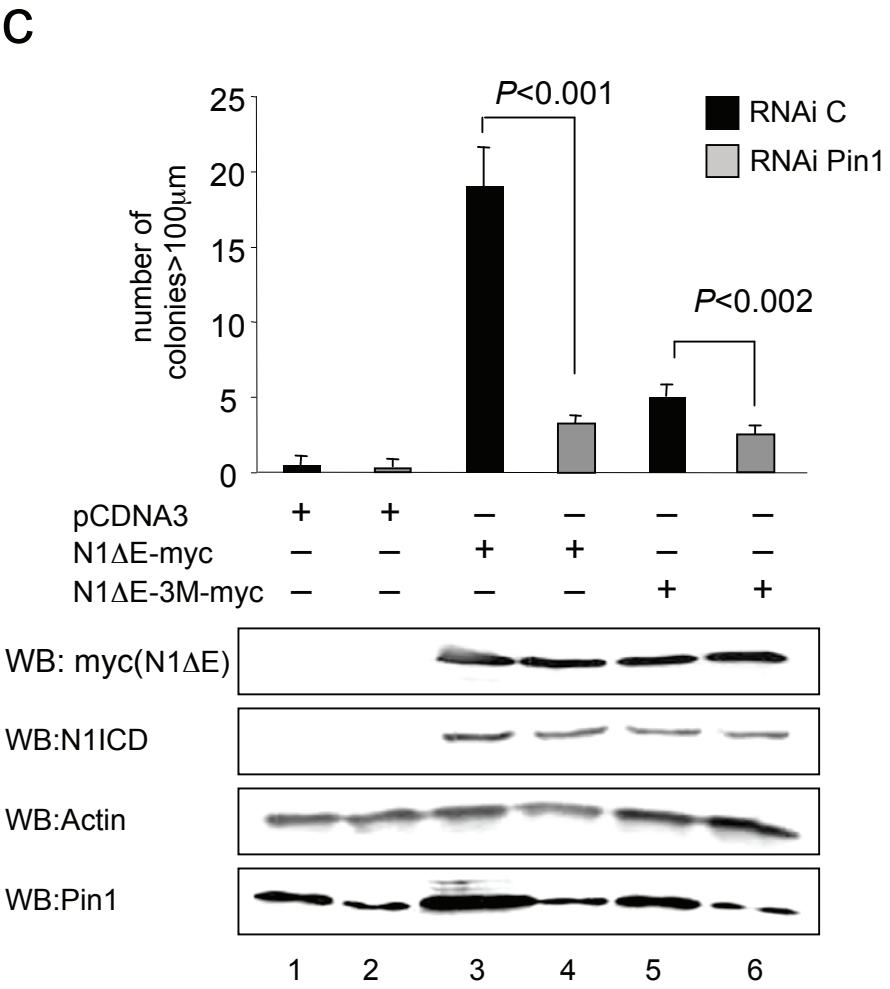

Figure S4 continued

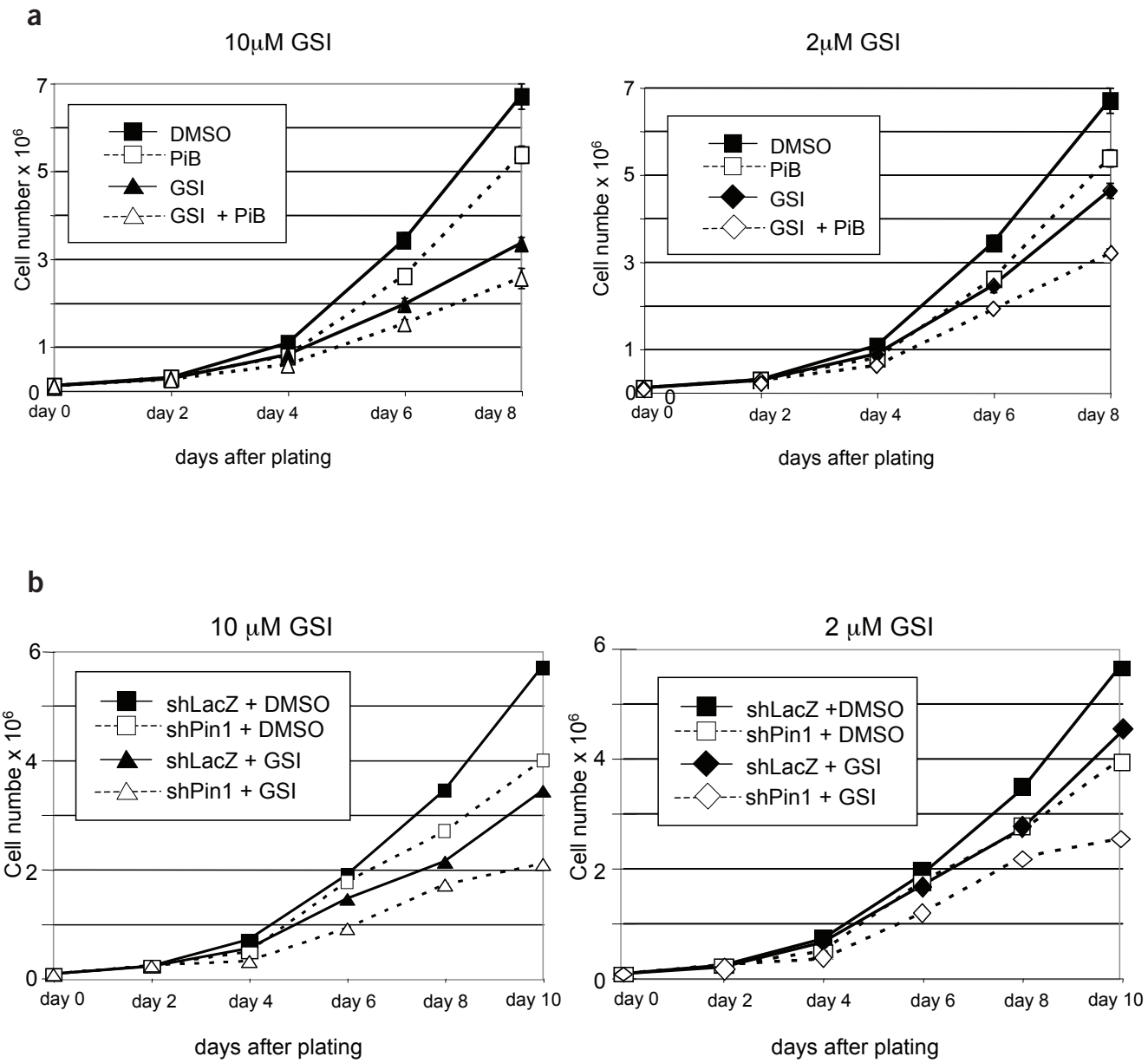

Figure S5 Inhibition of Pin1 catalytic activity sensitizes breast cancer cells to γ-secretase inhibitor treatment. **a)** Effect of co-administration of Pin1 and γ-secretase small molecule inhibitors on growth of breast cancer cells. Graphs show growth curve of MDA-MB-231 breast cancer cells treated with 10 (left panel) or 2 μM GSI (right panel) and with PiB (open symbols) or DMSO (black symbols). Cells were counted every two days for 8 days after plating. Graphed are the means and s.d. of three independent experiments performed in duplicate each. *P*(DMSO vs. 10 μM GSI)<10^{-4}; *P*(DMSO vs. PiB)<10^{-4}; *P*(2 μM GSI vs. 2 μM GSI + PiB)< 10^{-4}; (student's t-test). **b)** Effect of Pin1 ablation on GSI induced growth reduction of breast cancer cells. Graphs show growth curve of MDA-MB-231 breast cancer cells treated with 10 (left panel) or 2 μM GSI (right panel) and with shPin1 (open symbols) or shControl (black symbols). Cells were counted every two days for 10 days after plating. Graphed are the means of one experiment performed in duplicate.

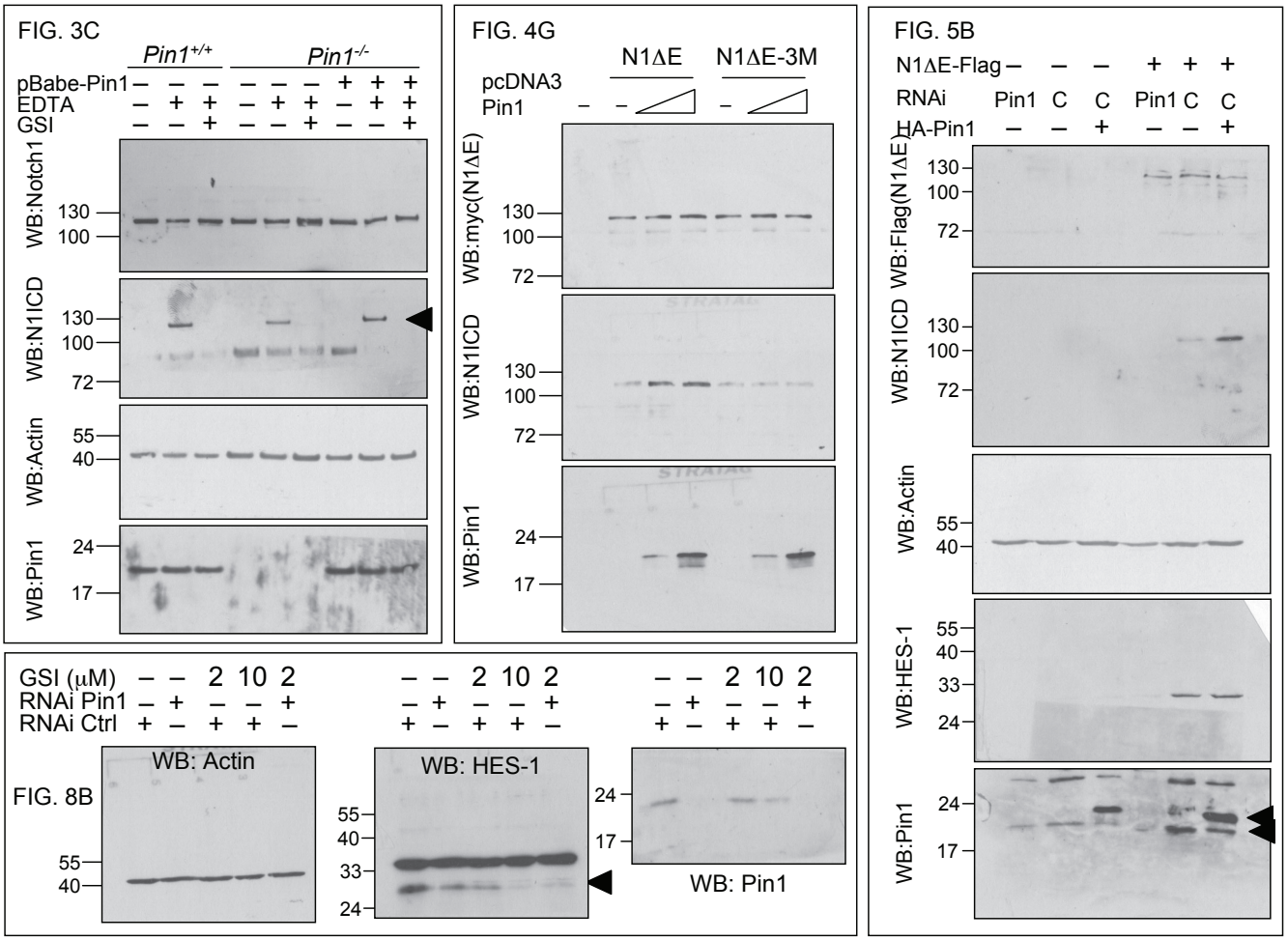

Figure S6 Complete scans of selected Western blots. For each panel, the corresponding figure shown in the manuscript is indicated on the top. Position of Molecular size markers (KDa) is indicated.

Supplementary Methods

Oligonucleotides. All oligonucleotides were purchased from MWG Biotech.
for cloning the human Pin1 promoter:
Forward primer 5'-AGGACGTGGAAGGCCTT-3' (713 bp upstream from ATG)
Reverse primer 5'-GCTGCGGCTCATGCGCT-3' (53 bp downstream from ATG)
for cloning pBabe-N1ΔE-myc:
Forward primer 5'GAGCGGATCC**ATG**CCGCCGCTCCTGGCGCCCCT-3' (BamHI site underlined and ATG initiation codon in bold print)
Reverse primer 5'-CATCCTTCTCGAG**CTT**GAAGGCCTCCGGAATG-3' (XhoI site underlined, no STOP codon, only last aa = E2555 of human Notch1 in bold print).
for construction of pBabe-N1ΔE-myc deletion plasmids (dP, d2171, d2120, dSTR, dSTR-dP):
At the 5' end the same forward primer as for pBabe- N1ΔE-myc was used.
At the 3' end the following reverse primers were used:
for dP and dSTR-dP 5'-TGGCTCGAGGTCTGCCTGGCTCGGCTCTCCACTCAGGA-3',
for d2171 5'-CTTCTCGAGCTTGCTTCCACAGGCCA-3',
for d2120 5'-CGGCTCGAGCACCAGGTTGTACTCGTCCA-3'
for internal truncations in constructs dSTR and dSTR-dP:
reverse primer on aa 2120 (5'-CGGGCTGTCGACCAGGTTGTACTCGT-3')
forward primer on aa 2175 (5'-GAGGCCGTCGACCTCAAGGCACGGA-3')
for construction of d2171-4M:
S2122A forward 5'-AGTACAACCTGGTGCGCGCCCCGCAGCTGCA-3'
S2122A reverse 5'-GCGCACCAGGTTGTACTCGTCCAGCA-3';
T2133A forward 5'-GAGCCCCGCTGGGGGGCGCGCCCACCCTGT-3'
T2133A reverse 5'-GCCCCCCAGCGGGGCTCCGTGCAGCT-3';
T2133A/S2137A forward 5'-GAGCCCCGCTGGGGGGCGCGCCCACCCTGGCGCCCCCGCTCT-3'
T2133A/S2137A reverse 5'- GCCCCCCAGCGGGGCTCCGTGCAGCT-3'
T2133A/S2137A/S2142A forward 5'-TGGCGCCCCCGCTCTGCGCGCCCAACGGCT-3'
T2133A/S2137A/S2142A reverse 5'-GCAGAGCGGGGGCGCCAGGGTGGGCGC-3'.
for generation of pcDNA3-HA-Pin1-S67E by site-directed mutagenesis:
Forward primer 5'- CTGGCTGTGCTTCACCAGCAGGTGCGAGCAG-3'
Reverse primer 5'-AGGGCCGCCGTTCCTGGCTGTGCTTCACCAGCA-3'
for RT-PCR:
HES-1 forward: 5'-GAGAAAAGACGAAGAGCA-3'
HES-1 reverse: 5'-TGTGCTCAGCGCAGCCGT-3'
HEY-1 forward: 5'-GAGGTGGAGAAGGAGAGTGC-3' [1]
HEY-1 reverse: 5'-CTCCGATAGTCCATAGCAA-3' [1]
PIN1 forward: 5'-CATCACTAACGCCAGCCAGT-3'
PIN1 reverse: 5'-TCAAATGGCTTCTGCATCTG-3'
GAPDH forward: 5'-GCCAGTGGACTCCACGAC-3'
GAPDH reverse: 5'-CAACTACATGGTTTACATGTTC-3'
for silencing:
siRNA Pin1(I) 5'-GCCAUUUGAAGACGCCUCG-3' [2]
siRNA Pin1(II) 5'-CGGGAGAGGAGGACUUUGA-3' (upgrade 7 from smart pool, Dharmacon)
siC(I) 5'-CCUUUUUUUUUGGGGAAAA-3' [2]
siC(II) 5'-GUGACCAGCGAAUACCUGU-3' (siRNA for LacZ [3])
shPin1 5'-GCCATTTGAAGACGCCTCG-3' (from siRNA Pin1(I))

shC (II) 5'-GTGACCAGCGAATACCTGT-3' (from siRNA LacZ) [3])
RISC-free control siRNA, Dharmacon.
for ChIP analysis:
BS1 forward 5'-AAAGTTGAGCCCTGCAAAAA-3' (677 bp upstream from ATG)
BS1 reverse 5'-AGGCGGGATAGAGCTTATGG-3'; (364 bp upstream from ATG)
BS2 forward 5'-AGAAGGGGTCGGGAGTTTT-3' (336 bp upstream from ATG)
BS2 reverse 5'-GCTGCCTATTGGCTAGACG-3' (69 bp upstream from ATG)

Plasmids. pcDNA3-N1ΔE-Flag, pBabe-N1ΔE-myc and deletion constructs for mapping studies, pcDNA3-d2171-myc and pcDNA3-d2171-3M(-4M), pcDNA3-N1ΔE-3M, pcDNA3-N1ICD-myc, pcDNA3-N1ICD-dSTR as well as pWZL-N1ΔE-Flag, pLPC-HA-Pin1 retroviral expression vectors were generated by standard procedures and details appear below. pBabe-Pin1, pGL2-HES-1/LUC and pBabe-ER/N1ICD-myc have been described[4-6]. For RNAi, sequences of oligonucleotides for shDNA cloned into pSuper.Retro (OligoEngine) are described above.
N1ΔE proteins were expressed using pcDNA3-N1ΔE-Flag and a series of derived constructs. It was obtained from human full length Notch1 (pBabe/HA-hNotch1 [7]) that was cloned into EcoRI site of pcDNA3 in frame with a Flag-tag at the C-terminus, then to obtain pcDNA3-N1ΔE a PCR-mediated in-frame deletion of aa 24-1714 was performed. An HA-tag was then inserted at aa 1731. pBabe(Puromycin)-N1ΔE-myc was generated starting from pcDNA3-N1ΔE-Flag by PCR and subcloning into BamHI and XhoI digested pBabe and pcDNA3 (Invitrogen) vectors bearing in frame a myc tag followed by two STOP codons 3' to the XhoI restriction site. pBabe-dP, -d2171, -d2120, -dSTR, -dSTR-dP were gereated by PCR starting from pBabe-N1ΔE-myc. For internal truncations in constructs dSTR and dSTR-dP a SalI restriction site at aa 2175 was exploited to design one reverse annealing primer on sequence corresponding to aa 2120 and one forward primer starting from that of aa 2175 (both containing a SalI restriction site) that were used in combination with the forward and reverse primers of pBabe-N1ΔE-myc, respectively. After SalI restriction the PCR products (corresponding to N-terminal to aa 2120 and of aa 2175 to the C-terminal end) were united by ligation-mediated PCR using again forward and reverse oligonucleotides of pBabe-N1ΔE-myc. pcDNA3-d2171-myc was generated by subcloning from pBabe-d2171-myc. Construction of pcDNA3-d2171-4M-myc started from pcDNA3-d2171-myc by introducing sequentially Serine (S) or Threonine (T) to Alanine (A) substitution one after the other by site-directed mutagenesis (OligoEngine). pWZL(Hygromycin)-NdE-Flag was obtained from pcDNA3-N1ΔE-Flag by PCR and subcloning. Retroviral vector pLPC(Puromycin)-HA-Pin1 was constructed by subloning from pcDNA3-HA-Pin1[2]. pcDNA3-HA-Pin1-S67E was obtained by site-directed mutagenesis from pcDNA3-HA-Pin1 [2]. pGL3-hPin1/LUC was constructed by subcloning a PCR product containing the human Pin1 promoter from HeLa genomic DNA into pGL3 (Promega). All constructs were checked by sequencing.

Antibodies for Western blot and Immunoprecipitation. The following antibodies were used: mouse monoclonal anti-MPM-2 (Upstate), rabbit and goat polyclonal anti-Notch1 (SantaCruz), rabbit polyclonal anti-N1ICD Val1744 (Cell Signaling), mouse monoclonal anti-myc clones 9E10 and 9B11 (Cell Signaling), mouse monoclonal anti–Flag and anti-HA (Sigma), rabbit polyclonal[4] and mouse monoclonal (SantaCruz) anti-Pin1, rabbit polyclonal anti-HES-1[8], anti-phosohErk1/2, anti-Erk1/2, anti-phospho-c-jun and anti-c-jun were from Cell Signaling.

Retroviral infection. Ampho/Phoenix packaging cells were transfected with indicated retroviral vectors by a standard calcium phosphate method. After 48 h incubation at 32°C, the supernatants containing viral particles were collected, and infection was performed as described[4].

Soft-agar analysis. Cells from MCF-10A, MDA-MB-231 and SKBr-3 stable clones used for soft agar experiments were resuspended in a top layer of the corresponding culture mediums with 0.3% or 0.25% agarose (Gellyphor, Euroclone), respectively, at 10,000 cells per well in triplicate in 6-well plates and plated on a bottom layer of culture medium containing 1% agarose. Every 2 days fresh inhibitors (GSI, PiB or DMSO) were added. After three weeks the colonies were counted with a 20X objective on a Olympus CK30 microscope.

RNA extraction and reverse-transcription PCR. Total RNA was extracted with TRIzol (Invitrogen), and 1 μg was reverse-transcribed using SuperscriptIII reverse transcriptase and random primers (Invitrogen) following the manufacturer's instructions. For PCR all primers have been chosen or designed in order to anneal on different exons of the respective cDNA (HES-1 NM_005524; Hey1[1] (or HERP 2) AF232239; Pin1 NM_006221; GAPDH BC083511). PCR settings are available upon request.

Chromatin immunoprecipitation (ChIP). Cells were crosslinked with 1% formaldehyde for 15 min, neutralized with 125 mM glycine pH 2.5 and washed in PBS. Nuclei were prepared by hypotonic lysis (5mM Pipes pH 6.8, 85 mM KCl, 0.5% NP40) and centrifugation, and resuspended in RIPA-100 buffer (20 mM Tris/HCl, pH 7.5, 100 mM NaCl, 1 mM EDTA, 0.5% NP40, 0.5% deoxycholate, 0.1% SDS) with protease inhibitor cocktail (Sigma), 1 mM PMSF and phosphatase inhibitors (NaF 5 mM, Na_3VO_4 1 mM). Chromatin was sonicated by Bioruptor (Diagenode) to 500-1000 bp average fragment size and cleared by centrifugation. IP was performed overnight at 4°C with either 2 μg of a goat anti-Notch1 antibody (sc-23304; SantaCruz Biotech.) or as an unrelated control goat anti-GST (GE, Amersham) antibody at 4 °C. DNA-protein complexes were recovered by protein A/G PLUS-Agarose (SantaCruz Biotech.) and washed sequentially with RIPA-100 and RIPA-250 buffer and LiCl solution (10 mM Tris/HCl pH 8, 1 mM EDTA, 250 mM NaCl, 0.5% Na-deoxycholate, 0.5% NP40), then resuspended in TE, digested with 2U Dnase-free Rnase (Calbiochem) for 30 min at 37°C, and incubated overnight at 68°C with 300 mg/ml Proteinase K (NEB) in 0.5% SDS, 100 mM NaCl to digest proteins and reverse crosslinks. After purification by phenol-chloroform separation and ethanol precipitation, DNA was resuspended in H_2O and 1/10 volume was used for quantification. 1/10 of input chromatin was amplified as standard for each experiment. PCR products were resolved on 2% agarose gels, visualized by EtBr staining, and quantified with Kodak Digital Science 1d 2.0.2 software. PCR settings are available upon request.

Supplementary Methods References

1. Hopfer, O., Zwahlen, D., Fey, M. F. & Aebi, S. The Notch pathway in ovarian carcinomas and adenomas. Br J Cancer 93, 709-18 (2005).
2. Mantovani, F. et al. Pin1 links the activities of c-Abl and p300 in regulating p73 function. Mol Cell 14, 625-36 (2004).

3. Bossi, G. et al. Mutant p53 gain of function: reduction of tumor malignancy of human cancer cell lines through abrogation of mutant p53 expression. Oncogene 25, 304-9 (2006).
4. Zacchi, P. et al. The prolyl isomerase Pin1 reveals a mechanism to control p53 functions after genotoxic insults. Nature 419, 853-7 (2002).
5. Jarriault, S. et al. Signalling downstream of activated mammalian Notch. Nature 377, 355-8 (1995).
6. Ronchini, C. & Capobianco, A. J. Notch(ic)-ER chimeras display hormone-dependent transformation, nuclear accumulation, phosphorylation and CBF1 activation. Oncogene 19, 3914-24 (2000).
7. Aster, J. C. et al. Oncogenic forms of NOTCH1 lacking either the primary binding site for RBP-Jkappa or nuclear localization sequences retain the ability to associate with RBP-Jkappa and activate transcription. J Biol Chem 272, 11336-43 (1997).
8. Ito, T. et al. Basic helix-loop-helix transcription factors regulate the neuroendocrine differentiation of fetal mouse pulmonary epithelium. Development 127, 3913-21 (2000).

Supplementary Figures References

1.Lu, P.J., Zhou, X.Z.,Shen, M., and Lu, K.P. Function of WW domains as phosphoserine- or phosphothreonine binding modules. *Science **283***, 1325-1328 (1999).
2.Wolfe, M.S. The gamma-secretase complex: membrane-embedded proteolytic ensemble. Biochemistry 45, 7931-9 (2006).